Geol. Mag. **141** (3), 2004, pp. 257–286. © 2004 Cambridge University Press
DOI: 10.1017/S0016756804009094 *Printed in the United Kingdom*

The ophiolite-related Mersin Melange, southern Turkey: its role in the tectonic–sedimentary setting of Tethys in the Eastern Mediterranean region

OSMAN PARLAK* & ALASTAIR ROBERTSON†

*Çukurova Üniversitesi, Jeoloji Mühendisliği Bölümü, 01330 Balcalı, Adana, Turkey
†Grant Institute of Earth Science, School of GeoSciences, West Mains Road, University of Edinburgh, Edinburgh EH9 3JW, UK

(*Received* 13 May 2003; *accepted* 18 December 2003)

Abstract – The Mersin Melange underlies the intact Mersin Ophiolite and its metamorphic sole to the south of the Mesozoic Tauride Carbonate Platform in southern Turkey. The Melange varies from chaotic melange to broken formation, in which some stratigraphic continuity can be recognized. Based on study of the broken formation, four lithological associations are recognized: (1) shallow-water platform association, dominated by Upper Palaeozoic–Lower Cretaceous neritic carbonates; (2) rift-related volcanogenic–terrigenous–pelagic association, mainly Upper Triassic andesitic–acidic volcanogenic rocks, siliciclastic gravity flows, basinal carbonates and radiolarites; (3) within-plate-type basalt–radiolarite–pelagic limestone association, interpreted as Upper Jurassic–Lower Cretaceous seamounts with associated radiolarian sediments and Upper Cretaceous pelagic carbonates; (4) ophiolite-derived association, including fragments of the Upper Cretaceous Mersin Ophiolite and its metamorphic sole. Locally, the ophiolitic melange includes granite that yielded a K/Ar radiometric age of 375.7 ± 10.5 Ma (Late Devonian). This granite appears to be subduction influenced based on 'immobile' element composition.

The Mersin Melange documents the following history: (1) Triassic rifting of the Tauride continent; (2) Jurassic–Cretaceous passive margin subsidence; (3) oceanic seamount genesis; (4) Cretaceous supra-subduction zone ophiolite genesis; (5) Late Cretaceous intra-oceanic convergence/metamorphic sole formation, and (6) latest Cretaceous emplacement onto the Tauride microcontinent and related backthrusting.

Regional comparisons show that the restored Mersin Melange is similar to the Beyşehir–Hoyran Nappes further northwest and a northerly origin best fits the regional geological picture. These remnants of a North-Neotethys (Inner Tauride Ocean) were formed and emplaced to the north of the Tauride Carbonate Platform. They are dissimilar to melanges and related units in northern Syria, western Cyprus and southwestern Turkey, which are interpreted as remnants of a South-Neotethys. Early high-temperature ductile transport lineations within amphibolites of the metamorphic sole of the Mersin ophiolite are generally orientated E–W, possibly resulting from vertical-axis rotation of the ophiolite while still in an oceanic setting. By contrast, the commonly northward-facing later stage brittle structures are explained by backthrusting of the ophiolite and melange related to exhumation of the partially subducted northern leading edge of the Tauride continent.

Keywords: melange, ophiolite, Turkey, East Mediterranean, Tethys.

1. Introduction

Melanges associated with ophiolites shed light on the regional tectonic evolution of oceanic basins and continental margins (Gansser, 1974). Melanges play an important role in the tectonic evolution of Tethys in the Eastern Mediterranean region, especially in Turkey (Robertson, 1994). In southern Turkey, an E–W-trending Mesozoic shallow-water carbonate platform, known as the Tauride Carbonate Platform, is bounded to the north and south by allochthonous ophiolite-related units, including melanges (Fig. 1).

† Author for correspondence: Alastair.Robertson@glg.ed.ac.uk

The southern margin of the Tauride Carbonate Platform, locally known as the Bolkar Dağ (Fig. 2), is overthrust by melange and a dismembered ophiolite (Demirtaşlı *et al*. 1984; Dilek & Whitney, 1997; Parlak, Çelik & Delaloye, 2001). Along strike, further west, there are regionally extensive allochthons that include continental margin, basinal, ophiolitic and melange units and are known as the Beyşehir–Hoyran–Hadim Nappes (Özgül, 1984, 1997; Monod, 1977; Andrew & Robertson, 2002; Elitok, 2002). Further west again, extending to the Aegean coast are comparable marginal, basinal and ophiolitic units of the Lycian Nappes (De Graciansky, 1972; Poisson, 1977; Şenel, 1991; Collins & Robertson, 1997, 1998). In addition, broadly

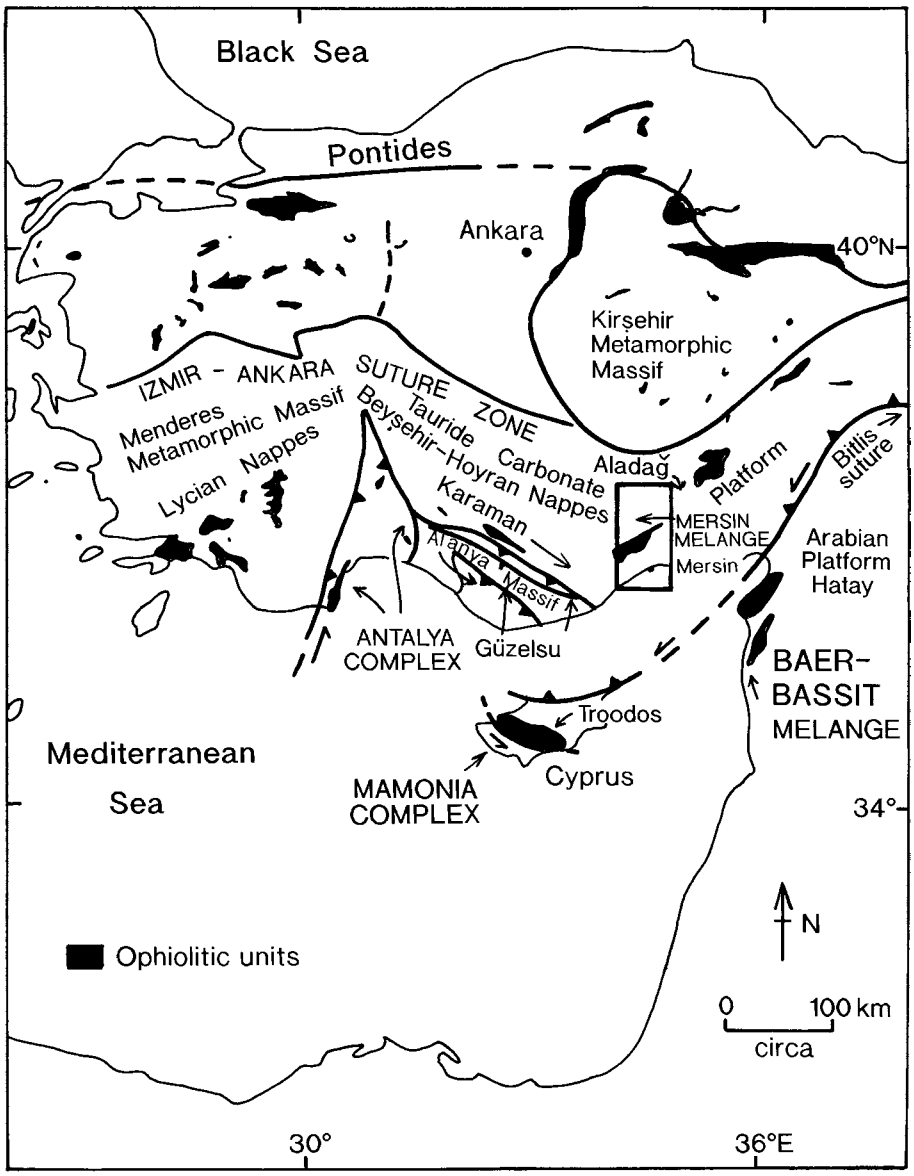

Figure 1. Outline tectonic map of western Turkey showing the Mersin Melange, and related tectonic units discussed in the text. Box indicates location of Figure 2.

similar ophiolitic units are exposed to the south of the Tauride Carbonate Platform in an elongate belt extending from eastern Turkey, through northern Syria (Baer–Bassit region), western Cyprus (Mamonia Complex), to southwestern Turkey (Antalya Complex; see Robertson, 2002, for a review).

In one interpretation, all of these allochthonous ophiolite-related units were thrust from a single Tethyan ocean basin, located to the north of the Tauride Carbonate Platform, during Late Cretaceous–Early Tertiary time (Ricou, Argyriadis & Marcoux, 1975). Alternatively, the northerly units (e.g. Beyşehir–Hoyran Nappes) were derived from one (or several) northerly oceanic basin (Northern Neotethys or Inner Tauride Ocean), whereas southerly units (e.g. Mamonia Complex, Antalya Complex) were derived from a separate southerly oceanic basin (Southern Neotethys) (Robertson & Woodcock, 1980; Şengör & Yılmaz, 1981). Recently, dual origins were assumed in several regional plate tectonic syntheses (Robertson, 1998, 2000; Stampfli *et al*. 2001).

The above interpretations have not taken into account melange and ophiolite exposures, known as the Mersin Melange and the Mersin Ophiolite, that are located to the south of the Tauride Carbonate Platform in the hinterland of the coastal city of Mersin (Fig. 2). Previous reconnaissance has suggested an origin of the melange and ophiolite as Mesozoic continental margin and oceanic units that were emplaced from the Southern Neotethys (Parlak, 1996; Parlak, Bozkurt & Delaloye, 1996). This interpretation is problematic, as it is generally assumed in most regional reconstructions

https://doi.org/10.1017/S0016756804009094 Published online by Cambridge University Press

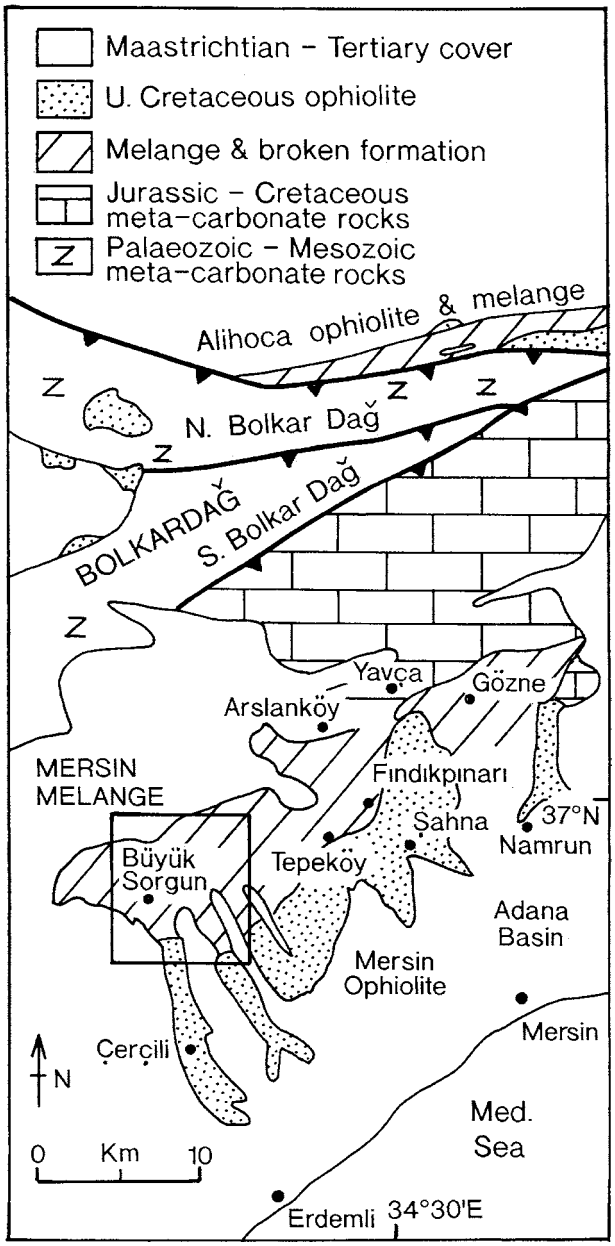

Figure 2. Simplified geological map showing the regional setting of the Mersin Melange. See Figure 1 for location. Box indicates location of Figure 4.

that northward subduction took place beneath the Tauride microcontinent from the Southern Neotethys (Hall, 1977; Aktaş & Robertson, 1984; Yılmaz, 1993; Robertson *et al*. 2004). On the other hand, southward emplacement of ophiolites onto the northern margin of the Tauride Carbonate Platform in the same region is now well established (Monod, 1977; Özgül, 1984, 1997; Andrew & Robertson, 2002).

In this paper, we will discuss the tectono-stratigraphy, structure and origin of the Mersin Melange in the light of other ophiolite-related melange units located both to the south and north of the Tauride Carbonate Platform.

2. Regional setting

The Mersin Melange forms a NE–SW-trending exposure, *c*. 40 km long by up to 15 km wide (Fig. 2). The best outcrops are on the southern flank of the Bolkar Dağ above the tree line (*c*. 1500 m). In the northeast, the Mersin Melange directly overlies Upper Cretaceous pelagic carbonates and ophiolite-derived debris flow units ('olistostromes'), forming the highest stratigraphic levels of the Tauride Carbonate Platform (the Southern Bolkar Dağ). Further west it is exposed in inliers beneath Miocene cover sediments of the Adana Basin, with no exposed base.

Mapping of two areas by Pampal (1984, 1987) established the following overall tectono-stratigraphy beneath the Tertiary sedimentary cover, from the top downwards: (1) Mersin Ophiolite; (2) metamorphic sole of the ophiolite; (3) Mersin Melange (Fig. 3). Metamorphic sole-type rocks are also locally preserved as dismembered blocks and slices within the Mersin Melange (Parlak, 1996; Parlak, Delaloye & Bingöl, 1995).

The Mersin Melange is structurally overlain by the Mersin Ophiolite, with a locally preserved metamorphic sole. Each of the units of a complete ophiolite (*c*. 6 km thick) are present within the Mersin Ophiolite with the exception of a sheeted dyke complex. The ophiolite is well exposed in several deep valleys dissecting the Miocene Adana Basin (Fig. 2), whereas the metamorphic sole is only well exposed in a few small areas (Parlak, 1996; Parlak, Delaloye & Bingöl, 1996, 1997).

3. Nomenclature

Melange is defined as blocks of heterogeneous lithologies set in an incompetent matrix (see Raymond, 1984), regardless of whether the melange is of sedimentary or tectonic origin, or both. Broken formation (AGI, 1961) comprises strongly deformed units in which some stratal coherence can still be recognized by mapping. Although given the regional name, Mersin Melange (Parlak, 1996), not all of the exposure conforms to melange, as defined above. Exposures of broken formation are also present in which locally coherent stratigraphic successions from tens to hundreds of metres thick are present.

4. Structure of the melange

The melange blocks and broken formation mainly strike NE–SW and dip southwards at moderate to rarely steep angles (Figs 4, 5a, b). This regional attitude was attained prior to covering by Early Tertiary shallow-marine carbonates (Avşar, 1992). The melange blocks typically range from tens of metres to several hundred metres in size, with competent limestone being the most prominent lithology. Many of the

https://doi.org/10.1017/S0016756804009094 Published online by Cambridge University Press

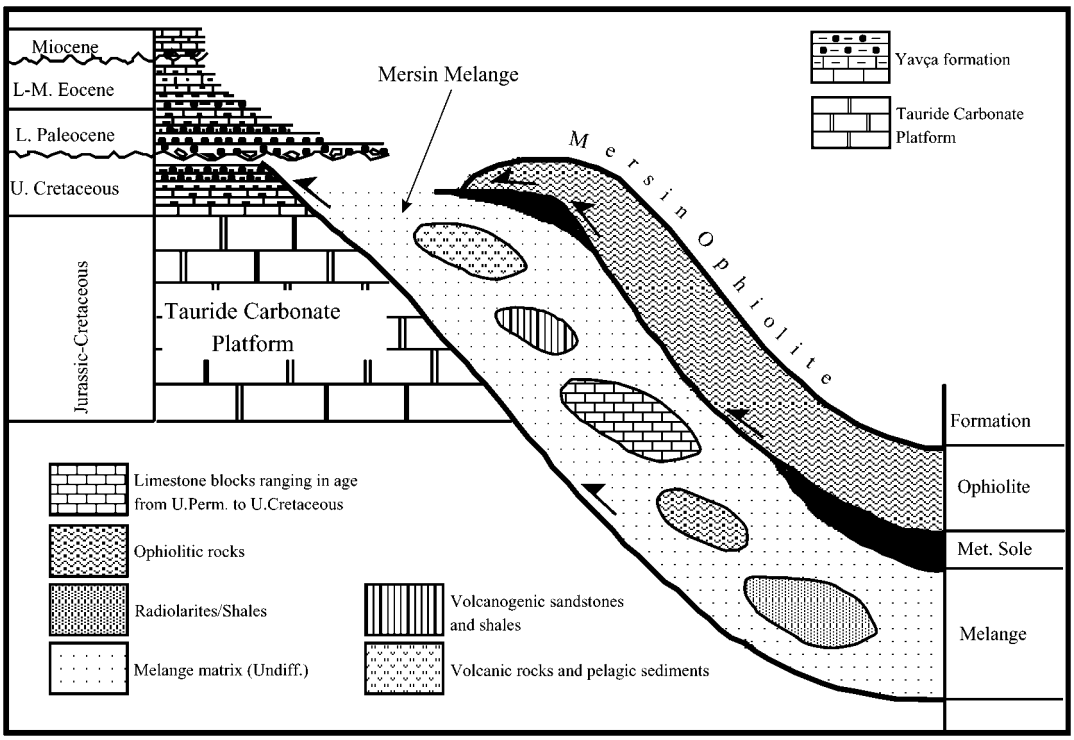

Figure 3. Tectono-stratigraphic setting of the Mersin Melange. See text for explanation.

limestone blocks are internally faulted and slickensided around the margins. Areas of broken formation are dominated by elongate internally disrupted thrust sheets. These are mainly limestones that range from hundreds of metres to several kilometres long. Internal deformation is restricted to common faulting and minor folding. Several areas (e.g. near Sorgun and Tepeköy; Fig. 2) were mapped as coherent bodies of Late Palaeozoic–Mesozoic, mainly carbonate rocks (Pampal, 1984, 1987). However, our observations show that most exposures comprise numerous smaller sheets and blocks, commonly separated by a poorly exposed melange matrix. In some areas, lithologically similar units are structurally repeated several times with a soft, fine-grained shaly matrix in between.

In a few places (e.g. Boyunyurt Tepe, near Gavuruçtuğu, Fig. 4), limestone broken formation is folded, with rare medium- to large-scale, inclined to isoclinal folds. Such folds typically verge northwards. On the other hand, where (very rarely) sedimentary way-up evidence could be observed in fold limbs (that is, grading and small-scale cross-bedding), several folds were inferred to face southwards (e.g. southeast of Büyük Sorgun). More commonly, folds show no preferred vergence (Fig. 5c).

We observed additional evidence of northward displacement near the contact between the ophiolite and the underlying melange (by the bridge on the Büyük Sorgun road, near Poyrazlı; Fig. 4). This melange dips at *c*. 45° southwards beneath the serpentinized mantle rocks of the Mersin Ophiolite. Near the contact, the ophiolite tectonites exhibit north-verging C-S fabrics. Further north towards Büyük Sorgun (Fig. 4), basalt-red chert-shale alternations exhibit small north-verging folds and duplex structures. Further south, opposite Çerçili (Fig. 2), radiolarite intercalations beneath the ophiolite are deformed into medium-scale north-verging isoclinal folds with sheared limbs. On the opposite (western) side of the river, similar lithologies contain numerous north-verging, inclined to isoclinal folds.

The southward regional dip and predominantly northward fold and thrust vergence, as confirmed during this study, were previously taken to indicate that the melange was emplaced from south to north, that is, from a southerly Neotethyan basin. This interpretation was mainly based on structural evidence from the metamorphic sole of the ophiolite (Parlak, Bozkurt & Delaloye, 1996). However, this hypothesis needs to be re-evaluated in terms of the stratigraphy and palaeo-environments represented by the melange and broken formation and the regional tectonic context. In addition, new structural evidence from the metamorphic sole, leading to a revised interpretation, is presented in Section 9.

5. Lithological associations

When lithological associations rather than individual blocks or dismembered thrust sheets are mapped (Hall, 1980), four distinctive assemblages are recognized (Fig. 6):

https://doi.org/10.1017/S0016756804009094 Published online by Cambridge University Press

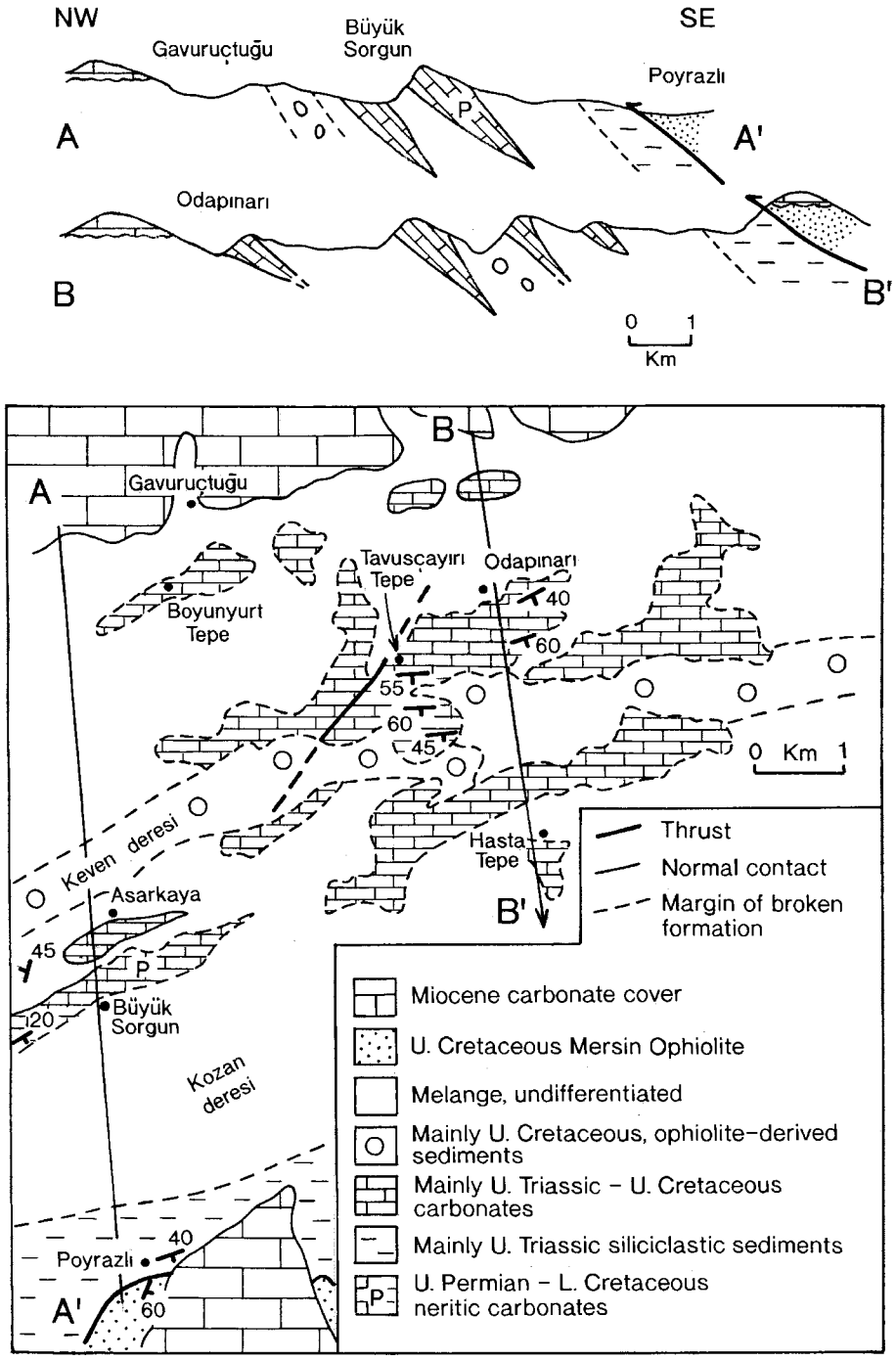

Figure 4. (bottom) Geological map of the westerly exposure of the Mesin Melange discussed in this paper, showing locations of cross-sections A–A′ and B–B′. (top) Simplified cross-sections of the Mersin Melange.

(1) shallow-water carbonate association;
(2) volcanogenic–terrigenous-pelagic association;
(3) basalt–radiolarite–pelagic limestone association;
(4) ophiolite-derived association.

Melange and broken formation of the shallow-water carbonate association (1) form hills rising several hundred metres above the general melange altitude (up to *c*. 1900 m). Although mapped as an over-riding thrust sheet by Pampal (1984, 1987), this unit dips regionally southwards and is interleaved with the matrix and other lithological associations of the melange. The volcanogenic–terrigenous–pelagic association (2), particularly its stratigraphically lower part, is well exposed in the south and dips beneath the Mersin Ophiolite. Similar lithologies also commonly occur as blocks throughout the melange. The basalt–radiolarite–pelagic limestone association (3) is located in the southwest and comprises sheared intercalations of basalt, radiolarite and hemipelagic limestone, with

https://doi.org/10.1017/S0016756804009094 Published online by Cambridge University Press

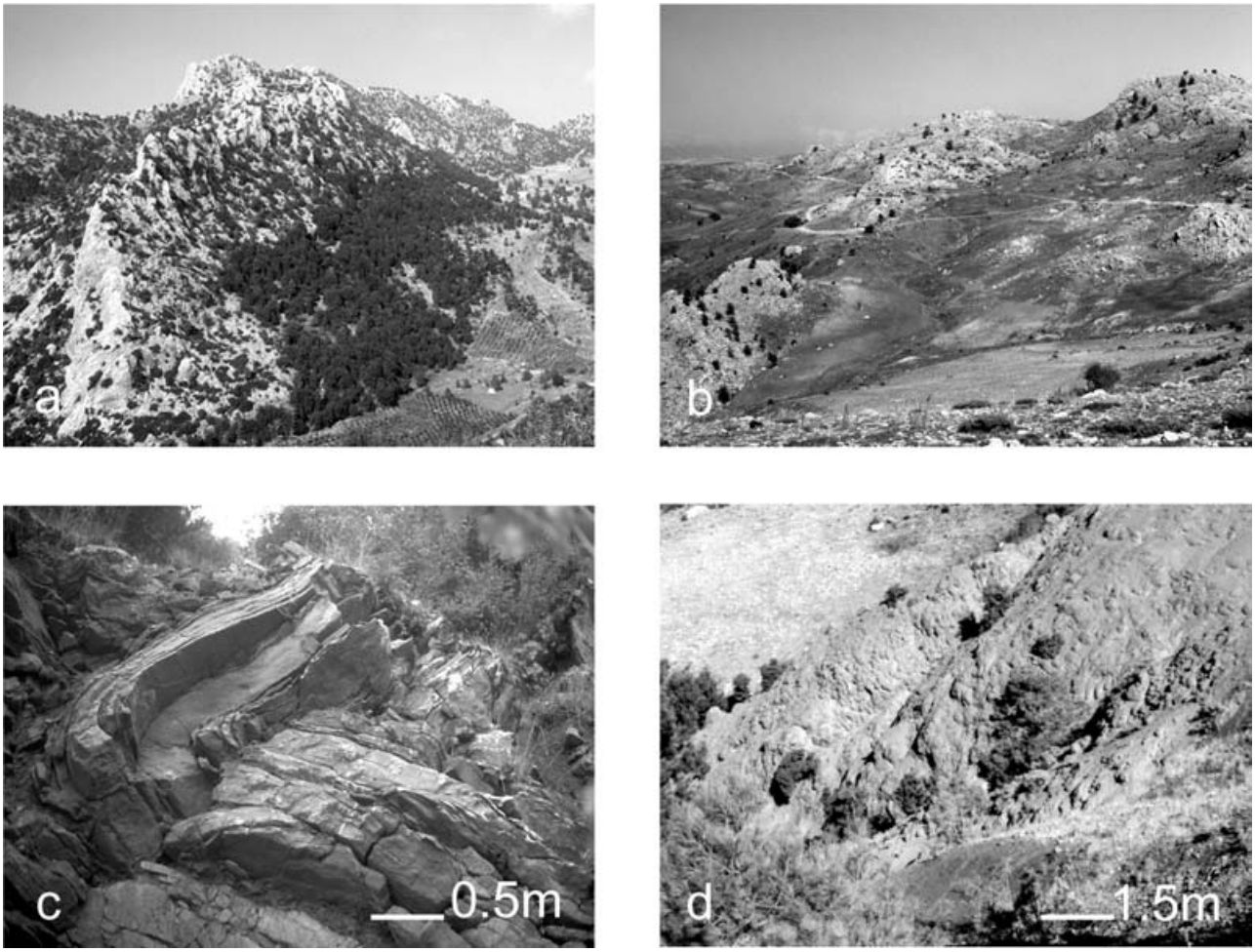

Figure 5. Field photographs of the Mersin Melange. (a) South-dipping grain of Permian–Triassic mainly neritic carbonates, Ziyaret Tepe area (north of Büyük Sorgun). (b) Typical exposure of melange mainly composed of south-dipping Triassic limestone blocks set in a poorly exposed matrix; Tavusçayırı Tepe area. (c) Triassic bedded limestone showing typical outcrop-scale folds lacking preferred vergence, Kozan deresi. (d) Pillow basalt from the base of the metamorphic sole, Fındıkpınarı (see Figs 2 and 4 for locations).

an aggregate thickness of up to several hundred metres. The largest exposures of the ophiolite-derived association (4) are in the south, directly beneath the Mersin Ophiolite. This unit also occurs as elongate thin units throughout the melange, commonly as soft-weathering material.

5.a. Shallow-water carbonate association

Relatively intact successions of Late Palaeozoic and Mesozoic age are recognized within broken formation, especially near Büyük Sorgun in the west and near Tepeköy, further east (Figs 2, 3). An overall Late Permian–Late Cretaceous shallow-water carbonate succession (Fig. 6, no. 1) is reconstructed, as follows:

Several exposures of broken formation form NE–SW-trending ridges (> 5 km long and up to 2 km wide; Fig. 5a) north of Büyük Sorgun (Fig. 4). The lower part of the succession, exposed several kilometres WSW of Büyük Sorgun, is dominated by well-bedded, dark calcarenite, passing upwards into thick-bedded to massive grey limestone (collectively termed the Göktepe Limestone by Pampal (1987, pp. 146–7). The dark, lower limestones yielded a fauna dominated by benthic foraminifera: *Baresella* sp., *Tetrataxis* sp., *Fusulinella* sp., *Agathammina* sp., *Pseudofusulina* sp., *Girvanella* sp., *Yangcheina* sp., *Parafusulina* sp., *Afghanella* sp., *Paleotextularia* sp., together with Schubertellidae, Schwageriniae and Neoschwageriniae. These microfossils are indicative of a Late Permian age. Limestones higher in the succession (included within the Göktepe Limestone) yielded *Involutina* sp., *Agathamina* sp., *Frondicularia woodwardii*, *Pseudoyclammina* sp., *Triasina* sp., *Trocholina* sp., *Opthalmidium* sp. and *Trochammina* sp., of non-specific Triassic to Early Cretaceous age (Pampal, 1984, p. 150). Traced northeastwards, the limestone exposure thins and is mapped as exclusively Mesozoic limestone to the north of Büyük Sorgun village. Where examined near the road south of the village, white micritic limestone, with replacement chert, is interbedded with grey calcarenite. White

https://doi.org/10.1017/S0016756804009094 Published online by Cambridge University Press

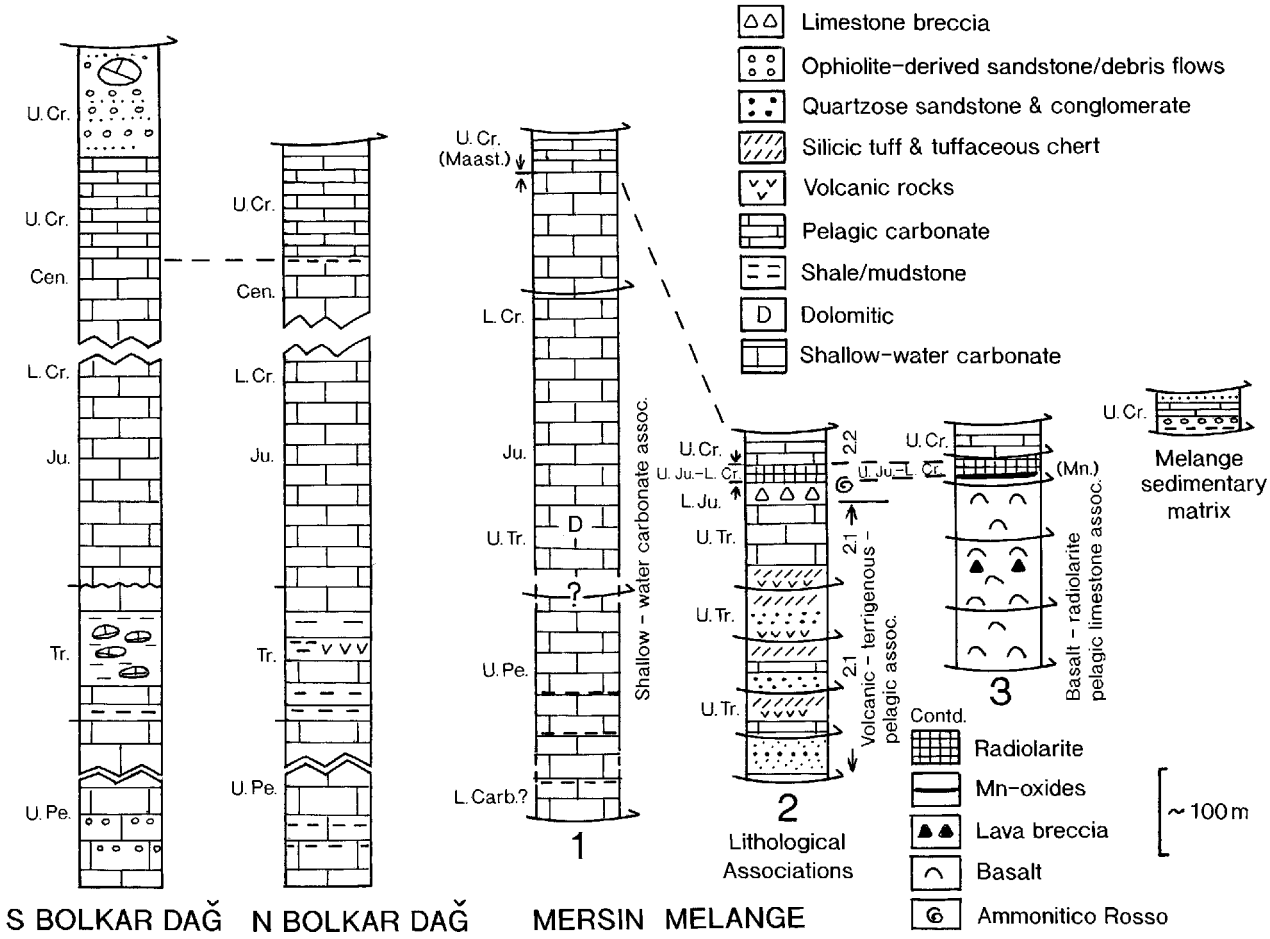

Figure 6. Generalized logs of the main lithological units exposed in the Bolkar Dağ (Northern and Southern units) and the Mersin Melange. The columns 1–3 are for the Mersin Melange, as follows: (1) shallow-water carbonate association; (2) volcanic–terrigenous–pelagic association; (3) basalt radiolarite–pelagic limestone association.

biomicrite containing coral and microbial carbonate is also exposed. In this area, large limestone blocks and broken formation are enveloped in sheared green tuff and silicic lava.

Elsewhere in the Büyük Sorgun area another dismembered sheet begins with dolomitic limestone (again attributed to the Göktepe Limestone). This contains a similar fauna, of inferred Permo-Triassic age. The succession passes into limestones that contain *Kurnibia* sp., *Lituosepta* sp., *Pseudolituonella* sp. and *Nautiloculina* sp., of inferred Triassic to Early Cretaceous age. Overlying thin- to medium-bedded limestones and grey massive limestone (assigned to the Kevençukuru Limestone by Pampal, 1987) include *Everthyclammina* sp., Litoulidae and algae, of inferred Early Cretaceous (Berriasian) age.

In a second area, broadly along-strike about 14 km to the northeast, several kilometres south of Tepeköy (Fig. 2), Late Palaeozoic–Mesozoic carbonate rocks were mapped as several large sheets of neritic limestone, up to several kilometres long (Pampal, 1984). These contain *Involutina* sp., *Opthalmilina* sp., *Meandrospira* sp., *Glomospirelia* sp., *Fondicularia* sp. and *Duotaxis* sp., indicative of a Late Triassic age.

Approximately 10 km north of Tepeköy, a zone of E–W-trending broken formation and blocks (near Arslanköy; Fig. 2) is dominated by neritic carbonates of Jurassic–Cretaceous age. Pampal (1984) reports a relatively intact succession, 750 m thick, of shallow-water carbonates (Çağıloluktepe Limestone), that has yielded *Ophthalmidium* sp., *Textularia* sp., *Pseudocyclammina* sp., *Pseodosyrisalidina* sp., *Pfenderina* sp. and Miliolidae. The succession passes conformably upwards into pelagic carbonates (Yavça Limestone), several tens of metres thick. A Late Campanian–Maastrichtian age is inferred from the planktic foraminiferal assemblage, *Globotruncana* cf. *stuarti*, *G. globigerinoides*, *G. lapperenti*, *G. bulloides*, *Globotrunca* sp. and *Heterohelix* sp.

5.a.1. Interpretation: pre-rift to post-rift shelf environments

An intact Upper Permian to Lower Cretaceous shallow-water carbonate succession was covered with Upper Cretaceous pelagic carbonates. The Early to Mid-Triassic interval may be largely absent owing to syn-rift flexural uplift, whereas the widespread Late Triassic neritic carbonates probably record the onset of post-rift

https://doi.org/10.1017/S0016756804009094 Published online by Cambridge University Press

subsidence after seafloor spreading began. Passive margin subsidence continued with further shallow-water accumulation on carbonate platform units until Late Cretaceous time, when subsidence and deep-water carbonate deposition ensued. The Permian–Late Cretaceous facies are similar to the southern part of the Bolkar Dağ and the Tauride Carbonate Platform in general (e.g. Poisson, 1977; Özgül, 1984; Fig. 6).

5.b. Volcanogenic–terrigenous–pelagic association

This lithological association comprises (1) a stratigraphically lower volcanogenic–terrigenous–limestone succession (Fig. 6, no. 2.1) and (2) a stratigraphically higher redeposited carbonate–radiolarite–pelagic carbonate succession (Fig. 6, no. 2.2). The first of these is dominated by disrupted, incompetent lithologies (e.g. shale; Fig. 8a). Some stratigraphic continuity can be seen, for example, in deep valleys northeast of Büyük Sorgun. This unit is considered as broken formation, since exotic rocks (e.g. ophiolite) or melange matrix (e.g. Upper Cretaceous debris flows) are absent. However, an unbroken succession cannot be determined. By contrast, the overlying redeposited carbonate–radiolarite–pelagic carbonate succession generally forms hilly regions dominated by relatively competent limestone broken formation in which intact successions can be measured.

(1) Volcanogenic–terrigenous–limestone succession. This lower unit is well exposed directly beneath the ophiolite (e.g. southeast of Büyük Sorgun and near Tavusçayırı Tepe; Fig. 4). Lithologies comprise silicic tuff, volcaniclastic siltstone–sandstone, quartzose-micaceous siltstone–sandstone (commonly plant-rich) and rare conglomerate, together with pelagic limestone (locally siliceous). Variable amounts of mainly siliceous extrusive rocks (*c*. 72 % SiO_2: O. Parlak, unpub. data) are also present, together with pelagic limestones of Late Triassic age. The hemipelagic limestones include *Meandrospira* sp., *Glomospira* sp., *Aulotortus* sp., *Frendicularia* sp., *Involutina* sp., *Duostominidae* and *Auloteritus* sp., as well as *Trochamina* sp. and calcareous algae, together indicative of a Late Triassic (Carnian–Norian) age, as determined by MTA palaeontologists (in Parlak, 1996).

At one locality, 3 km southeast of Büyük Sorgun (Kozan deresi; Fig. 4), the main lithologies are purple brown siltstones, fine-grained sandstone and massive sandstone, in beds up to several metres thick. Sand grains are well rounded and some facies are pebbly. Very coarse quartzose sandstone packed with well-rounded, white quartzitic clasts (up to 10 cm in size) are locally present. Medium-grained sandstones (protoquartzite) contain quite well-rounded quartz grains, quartzite lithoclasts, muscovite, plagioclase (rare) and bioclasts, especially echinoderm plates, cemented by calcite spar. There are also green, thin-bedded chert and rare dark shale with occasional carbonate concretions. Also present are red ribbon radiolarites, red shales and limestone intercalations containing lenses of white chert, of replacement origin. Similar lithologies are also exposed 3 km south of Büyük Sorgun (near Poyrazlı; Fig. 4), Thick-bedded, medium-grained quartzose sandstones (*c*. 30 m thick), again with quite well-rounded grains, are intersheared with thick-bedded calcarenite and sheared radiolarite at this locality.

Elsewhere, highly disrupted lithologies in a well-exposed stream-cutting at Keven deresi (Fig. 4) include deformed greenish silicic volcaniclastic sedimentary rocks, intermediate-composition lava (andesite), pebbly calcite cemented tuff, green siliceous tuff (tuffite) and green chert.

(2) Redeposited carbonate–radiolarite–pelagic carbonate succession. Green siliceous tuffs, near the top of the volcanogenic–terrigenous–limestone succession (1), are depositionally overlain by basinal facies including limestone, radiolarian chert and pelagic carbonate.

A laterally continuous sheet of broken formation begins with poorly exposed volcaniclastic sandstone and thin-bedded pelagic limestone (3 km east of Gavuruçtuğu; Figs 4, 7, no. 1), This limestone contains numerous dark grey concretions of diagenetic chert. The succession passes conformably upwards into well-bedded, grey pelagic limestone, *c*. 10 m thick, dated as Late Triassic by MTA palaeontologists (in Parlak, 1996). These limestones contain concretions and lenses of grey to black replacement chert. The succession becomes more siliceous upwards and passes into redeposited limestone with abundant bedded chert of replacement origin (see Price, 1977, for definition of chert types). There are also prominent intercalations of matrix-supported debris flows and intervals affected by slump folding. The succession ends with chaotic debris-flow deposits containing lithologies exposed in the underlying succession. Similar limestone debris flows and chert-clast-rich breccias are commonly associated with Late Triassic limestone throughout the area (Fig. 8b, d).

Elsewhere, near Tavusçayırı (Fig. 4) several sheets of pelagic limestone, dated as Late Triassic in age by MTA palaeontologists (in Parlak, 1996), are separated by green tuffaceous sediment, up to 20 m thick. The lower of these units begins with *c*. 60 m of grey pelagic limestone and passes upwards into pink limestone with beds of red replacement chert near the top (Fig. 7, no. 2). This is overlain by *c*. 1 m of pink pelagic Ammonitico Rosso, packed with ammonites and other fossils (Fig. 8c).

Several kilometres along strike to the northwest, near Boyunyurt Tepe, a lithologically similar, but unusually steeply dipping, succession begins with *c*. 30–40 m of well-bedded, grey platey limestone (similar to Halobia limestones), including *c*. 2 m of black limestone rich in reworked ooids and pisoliths. Above,

https://doi.org/10.1017/S0016756804009094 Published online by Cambridge University Press

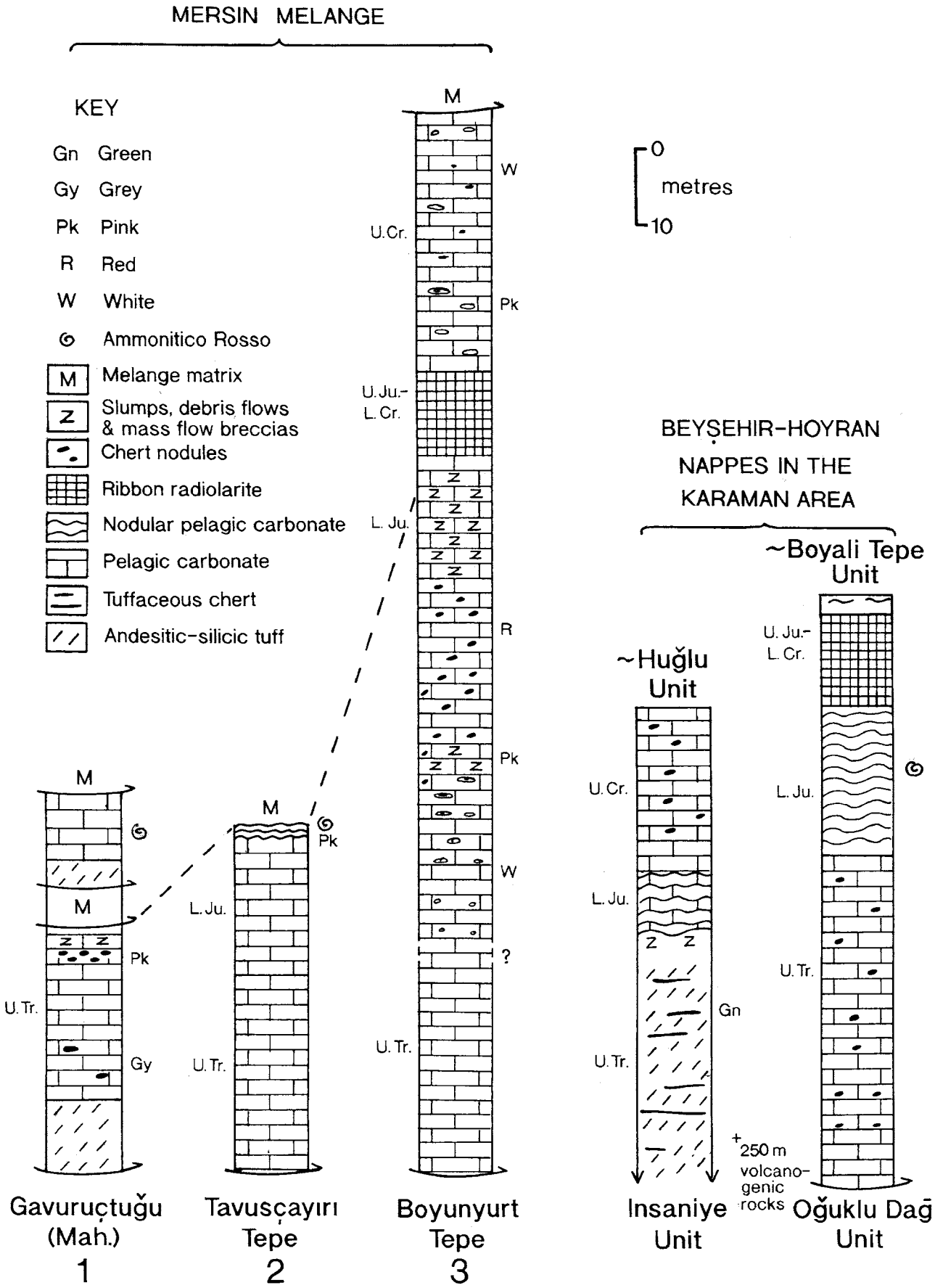

Figure 7. Detailed sedimentary logs of locally intact successions within the Mersin Melange. Logs of the correlative successions from the Beyşehir–Hoyran Nappes in the Karaman area (NW of the study area) are included for comparison; see text for explanation.

https://doi.org/10.1017/S0016756804009094 Published online by Cambridge University Press

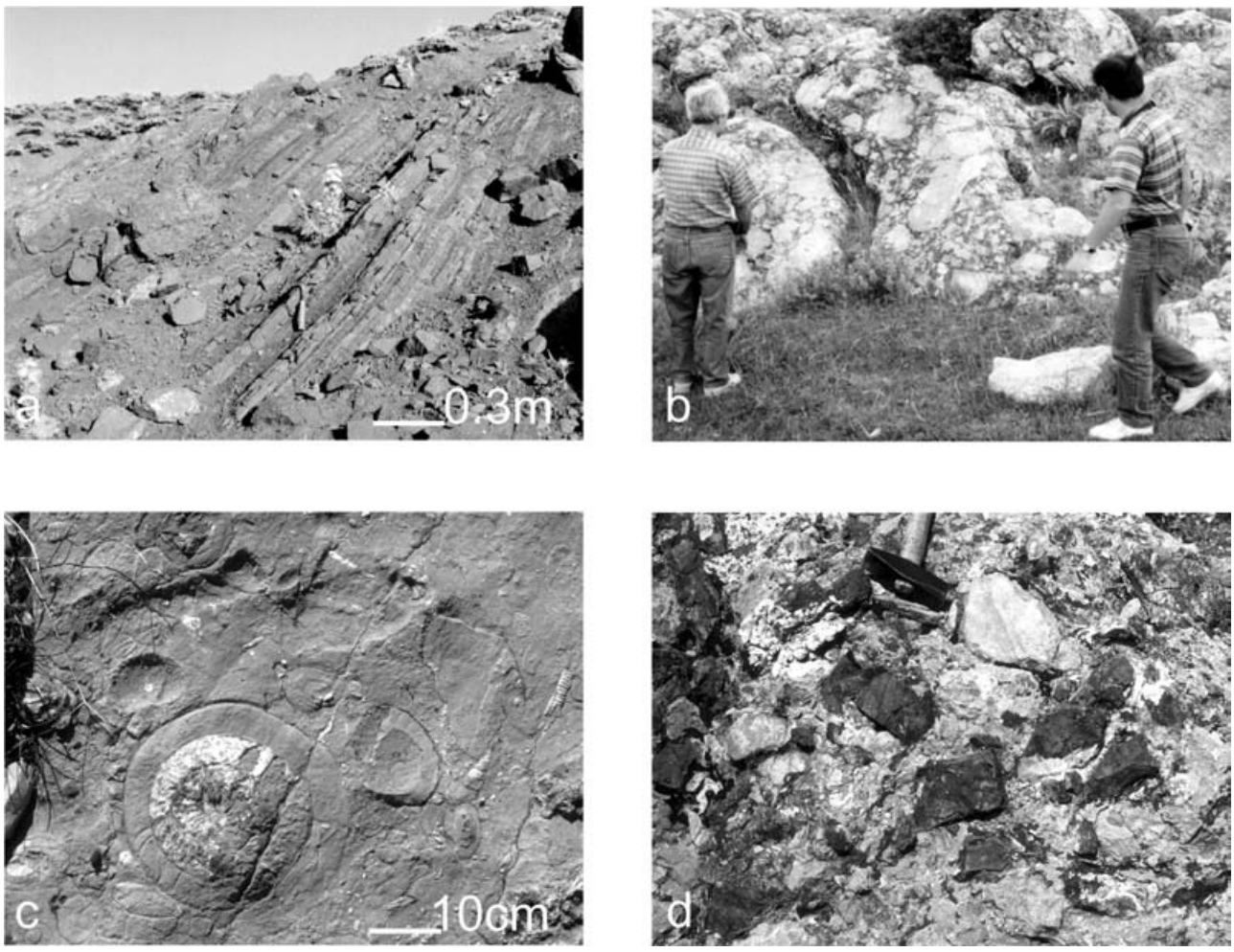

Figure 8. Field photographs of the Mersin Melange. (a) Well-bedded Triassic volcaniclastic sandstone and shale, Tepeköy area. (b) Limestone debris flow from above Upper Triassic neritic carbonate succession; Fındıkpınarı area. (c) Ammonitico Rosso from above Upper Triassic neritic carbonate succession, Tavusçayarı area. (d) Chert clast-rich breccias associated with debris flows from above Upper Triassic neritic carbonate succession; Fındıkpınarı area (see Figs 2 and 4 for locations).

an intact succession begins with *c*. 20 m of white, well-bedded, redeposited limestone with replacement chert. Above this, there is evidence of penecontemporaneous extension, creating irregular sheet-cracks into which red micrite has filtered. The succession continues with pink pelagic limestone, reddish nodular rubbly limestone (with abundant replacement chert) and limestone breccia, with clasts up to 1 m in diameter. This is followed by a *c*. 1 m thick layer of calcareous sandstone with reworked carbonate grains, partly replaced by silica. There is then a prominent interval of red ribbon radiolarite, several tens of metres thick, of inferred Late Jurassic–Early Cretaceous age, followed by *c*. 45 m of pink to white pelagic limestone with sparse planktic foraminifera and lenses of replacement chert in the lower part. Pampal (1987) reported Upper Cretaceous planktonic foraminifera from similar thin-bedded pink limestones within the melange.

Several large limestone blocks in the melange (e.g. near Tavusçayırı; Fig. 4) are dominated by sedimentary limestone breccia. Massive neritic limestone of Late Triassic age (dated by MTA palaeontologists; in Parlak, 1996) passes upwards into *c*. 10 m of limestone conglomerate and limestone breccia, implying gravity collapse. Neptunian sheet-cracks within these limestone breccias are infilled with pink micritic limestone.

Variable-sized blocks of limestone are scattered through the melange. For example, an isolated large block (in the Keven deresi area; Fig. 4) is dominated by angular to sub-angular clasts (up to 30 cm in size) of dark, fine-grained limestone containing reworked bioclastic material. Another block in the vicinity (40 m × 10 m) is composed of dark-coloured medium- to thick-bedded calciturbidites (in beds up to 1 m thick).

5.b.1. Interpretation: rift and subsiding deep-water passive margin

The lower part of the volcanogenic–terrigenous–pelagic association, of Late Triassic (Carnian–Norian) age, is interpreted as a deep-marine rift, infilled with a mixture of terrigenous, carbonate and volcanogenic

https://doi.org/10.1017/S0016756804009094 Published online by Cambridge University Press

material. The siliciclastic sediments were mainly deposited by turbidity currents and to a lesser extent by mass-flow processes. The source area included a metamorphic terrain, possibly now located beneath the Tauride Carbonate Platform. Mainly silicic-composition volcanic flows were locally erupted within the rift, coupled with an influx of large volumes of volcaniclastic sandstone turbidites and silicic air-fall tuff. Minor carbonate was redeposited from an adjacent shallow-water carbonate setting, presumably the Tauride Carbonate Platform. A relatively deep, open marine, setting is indicated by the presence of green radiolarian chert (mixed with tuff). Volcanism culminated with the accumulation of green tuffaceous deposits.

The rift basin was then covered by siliceous pelagic carbonate, in which chert formed diagenetically. The deep-water carbonates include calciturbidites, indicative of a slope setting. Increasing slope instability, probably related to continental break-up, culminated in large-scale slumping and mass flow-deposition. These disturbances mainly took place during Late Triassic time, associated with submergence of marginal carbonate platform units. Ammonitico Rosso accumulated locally on relatively stable submerged platforms (of latest Triassic age; G. Stampfli, pers. comm. 2004), whereas siliceous carbonate oozes and calciturbidites predominated in basinal areas. Radiolarian sediments accumulated widely in a relatively stable well-oxygenated deep-sea setting during Late Jurassic–Early Cretaceous time, when similar radiolarian sediments accumulated throughout the Eastern Mediterranean Tethyan region (De Wever, 1989). The probable control was high plankton productivity related to nutrient upwelling (Jenkyns & Winterer, 1982). Finally, the seafloor was blanketed with pelagic carbonate in Late Cretaceous time, prior to formation of the Mersin Melange.

5.c. Basalt–radiolarite–pelagic limestone association

In the southwest, the Mersin Ophiolite is directly underlain by intercalations of sheared basalt, radiolarite (Çerçili Radiolarite of Pampal, 1987) and hemipelagic limestone, with an aggregate thickness of up to several hundred metres (Fig. 6, no. 3). On the eastern slopes of the Büyük Sorgun river gorge, opposite Çerçili (Fig. 2), three radiolarite intercalations are present. It is unclear if these are stratigraphic or tectonic intercalations. Along a small road up the opposing (western) side of the stream valley, above Çerçili, radiolarites and red shales are interbedded with massive lava flows, pillow lava and lava breccia, in units up to 8 m thick. There are also pink pelagic limestones with lenses of red chert, formed by diagenetic replacement of carbonate. Occasional lenses of black pyrolusite, each up to tens of centimetres thick, are also present, together with widespread disseminated manganese oxide. Similar lithologies crop out elsewhere, especially in the southern part of the melange, for example, south of Büyük Sorgun, where massive basalt, red ribbon radiolarite and thin-bedded grey pelagic limestone are exposed along the road. Small exposures of similar lithological assemblages are seen within the melange. For example, sheared lozenges of red/purple sheared shale (e.g. exposed in Keven deresi; Fig. 4) include sub-rounded clasts of pelagic carbonate rock, basalt and chert.

5.c.1. Interpretation: within-plate oceanic basalts and pelagic sediments

The basalts are interpreted as small extrusive mounds formed on oceanic crust; these topographic highs were preferentially accreted into the melange, whereas underlying oceanic crust was subducted. These extrusives may be coeval with the Upper Jurassic–Lower Cretaceous cherts elsewhere in the melange, or with the Upper Cretaceous pelagic carbonates of the redeposited carbonate–radiolarite–pelagic carbonate succession, discussed in Section 5.b. Pampal (1987) reported the presence of *Hedbergella* sp. and *Ticinella* sp., of Late Cretaceous age, from pelagic limestones in the type area of the volcanic rocks, near Çerçili. A Late Cretaceous age for these radiolarites is presently inferred but needs to be confirmed with additional biostratigraphic studies in future. Eruption of the basalts was followed by accretion into the melange below the over-riding ophiolite. Similar volcanic rocks, also associated with manganese-oxide deposits of hydrothermal origin, were, for example, reported from an emplaced accretionary prism related to the sutured Pindos ocean in the northwest Peloponnese, Greece (Robertson & Degnan, 1998). Chemical data for the basalts will be presented in Section 7.

5.d. Ophiolite-derived association

Some areas of the Mersin Melange are dominantly ophiolitic. Lithologies include sheared, serpentinized harzburgite, layered and isotropic gabbro and altered basalt. There are also occasional dismembered thrust sheets and blocks of metamorphic rocks, including amphibolite, amphibolitic schist, quartz-mica schist, calc-schist and marble, correlated with the metamorphic sole of the Mersin Ophiolite. For example, large blocks and slices of ophiolitic units are present in a NE–SW-trending area, between Asarkaya and Tavusçayırı (Fig. 4). NE–SW-trending, ophiolite-derived broken formation, near Tavusçayırı, comprises ophiolitic basalt, sheared cumulate gabbro and includes one or several blocks of sheared granite (*c*. 10 m in size), set within serpentinized harzburgite. Elsewhere, in Keven deresi (Fig. 4), the melange is cut by a disrupted thrust sheet of sheared serpentinite, which includes a block of massive ophiolitic gabbro (7 m × 5 m) and disrupted amphibolite (*c*. 300 m long × 25 m wide).

https://doi.org/10.1017/S0016756804009094 Published online by Cambridge University Press

5.d.1. Interpretation: emplaced oceanic crust and metamorphic sole

The dismembered ophiolitic rocks in the melange are correlated with parts of the Mersin Ophiolite and its metamorphic sole. They were possibly detached from the leading edge of the over-riding ophiolite thrust sheet and imbricated into the underlying melange. Competent lithologies (e.g. amphibolite and gabbro) commonly form inclusions within sheared serpentine. In places, ophiolitic material was exposed on the seafloor and reworked as debris flows. For example, serpentinitic debris flow deposits include scattered clasts of red radiolarian chert and basalt, up to several metres in size (e.g. at Keven deresi; Fig. 4).

6. Matrix of the Mersin Melange

Two types of melange matrix are present in different parts of the melange, of both sedimentary and tectonic origin.

6.a. Sedimentary matrix

The sedimentary matrix is mainly debris flows and high-density lithoclastic turbidites, interbedded with hemipelagic carbonates (Fig. 6). These lithologies occur at specific horizons in the melange, commonly as deformed units, up to tens of metres thick. Polymict debris-flow deposits exposed at Keven deresi (Fig. 4) include pebbles, cobble and boulders (average 15 cm size) of medium-grained sandstone turbidites (locally with flute casts), conglomerate (with well-rounded clasts preserved), lava and radiolarite. Some of the radiolarite is recrystallized to red jasper. The margins of some of the limestone blocks are slickensided.

Elsewhere, the sedimentary matrix includes thin-bedded volcanogenic sandstones, weakly size-graded conglomerates, dark shales, radiolarites, radiolarian mudstones and siliceous pelagic limestones (Başpınar Formation of Pampal, 1987; e.g. 8 km west of Büyük Sorgun). Pelagic limestones in this areas have yielded *Hedbergella* sp. and *Ticinella* sp., of Late Cretaceous (Cenomanian) age. Elsewhere, *Dicyclina* sp., *Rotalia* sp., *Pseodolituonella* sp. and *Valvulammna* sp. were recorded, of Late Cretaceous (Santonian–Campanian) age. Interbedded hemipelagic matrix sediments contain *Globotrunca arca* and *G. calciformis*, of Late Cretaceous (Maastrichtian)–Early Paleocene age (Pampal, 1987). Pampal (1984) also reports that the melange matrix at Tepeköy (Fig. 2) contains the planktonic foraminifera *Globotruncana* sp., and *Globerigerina* sp., of Late Cretaceous–Paleocene age, together with benthic foraminifera *Textularia* sp., Rotaliidae, Miliolidea and Lagenidae) and Radiolaria.

6.b. Tectonic matrix

In some parts of the melange a sedimentary matrix is absent and the matrix is instead dominated by blocks (typically up to metre-sized) that are correlated with each of the four mappable lithological associations discussed above. Within individual areas the blocks can often be related to a single lithological association, as indicated by study of thin sections of blocks from Keven deresi (Fig. 4). A block of redeposited limestone there includes *Halobia* shell fragments, other bivalves, micritic grains and intraclasts of radiolarian micrite, and can be correlated with more intact Late Triassic successions elswhere in the melange. Bioclastic limestone blocks contain shell fragments, benthic foraminifera, microbial carbonate, pisoliths and micritic intraclasts. Another block includes shell fragments, echinoderm plates, thin-walled bivalves, iron-oxide-rich pellets, polyzoan fragments and small geopetals. These blocks correlate with Late Triassic-aged redeposited limestones forming more intact successions within the melange. In addition, common blocks of red fine-grained limestones originated as radiolarite within a calcareous and ferruginous matrix. All of the above blocks can be correlated with the redeposited carbonate–radiolarite–pelagic carbonate lithological association, described earlier. Similarly, in other areas of the melange the matrix can be correlated with one or another of the four lithological associations without any exotic material in these areas.

6.b.1. Interpretation: tectonic–sedimentary origin

The sedimentary matrix accumulated as debris-flow deposits, sandstone turbidites and hemipelagic mudstones in a deep-marine setting, probably a subduction trench, or 'fore-arc basin' within an accretionary prism. The original lithological successions were tectonically fragmented forming clasts, which were then resedimented into the deep-sea sediments as polymict debris-flow units and detached blocks. These sedimentary units were later incorporated into the melange as deformed thrust slices, forming parts of the matrix. Elsewhere, the former lithological successions were pervasively sheared to form blocks, but without undergoing resedimentation. The fine-grained matrix between these blocks is tectonic in origin. The melange matrix as a whole, therefore, formed by a combination of tectonic and sedimentary processes during latest Cretaceous time.

7. Basic extrusive igneous rocks

7.a. Petrography

Pillowed and massive volcanic rocks of the Mersin Melange range from basalt to andesite. The basalts display aphanitic, microlitic to microlitic porphyric

https://doi.org/10.1017/S0016756804009094 Published online by Cambridge University Press

Table 1. Representative major (wt %) and trace element (ppm) contents of the volcanic rocks in the Mersin Melange, southern Turkey

	Basalts						Basaltic andesites/Andesites								
Sample	OP-1	OP-5	OP-8	OP-15	OP-22	OP-348	OP-9	OP-18	OP-23	OP-26	OP-27	OP-31	OP-32	OP-362	OP-364
SiO_2	46.07	46.09	47.02	51.96	51.95	48.17	53.11	58.56	52.70	53.43	53.22	57.12	52.61	59.72	58.65
TiO_2	1.61	1.49	1.32	1.54	1.55	1.58	1.50	1.34	1.36	1.44	1.55	1.43	1.35	1.17	1.23
Al_2O_3	14.11	13.07	15.26	14.14	14.40	14.04	13.87	13.56	14.02	14.57	14.42	14.93	14.68	13.31	13.79
FeO^*	14.45	13.01	11.29	12.58	13.36	13.48	12.27	10.65	11.65	12.06	13.52	10.23	13.41	10.12	11.25
MnO	0.21	0.23	0.14	0.20	0.19	0.17	0.21	0.19	0.15	0.17	0.17	0.16	0.16	0.08	0.09
MgO	4.47	4.38	2.26	3.95	3.31	3.47	4.15	3.14	4.15	3.91	3.98	3.37	4.29	2.82	3.15
CaO	5.24	6.92	7.30	5.08	6.04	6.13	4.93	3.49	5.10	4.94	4.12	4.05	4.05	4.51	3.37
Na_2O	5.01	4.76	6.03	4.87	5.21	5.10	4.64	4.63	5.23	6.35	5.54	6.46	6.01	6.18	6.42
K_2O	0.28	0.19	0.49	0.07	0.02	0.28	0.09	0.15	0.02	0.05	0.20	0.21	0.16	0.21	0.22
P_2O_5	0.17	0.15	0.13	0.12	0.12	0.17	0.12	0.13	0.11	0.13	0.15	0.17	0.11	0.22	0.22
LOI	8.04	9.39	8.00	5.21	3.34	7.95	5.10	3.85	4.93	2.54	2.91	1.46	2.95	2.34	1.47
Total	99.67	99.68	99.24	99.72	99.48	100.55	100.00	99.70	99.43	99.59	99.78	99.58	99.77	100.70	99.87
Nb	3	3	1	2	1	5	2	2	2	3	3	2	1	7	6
Zr	95	93	89	94	83	93	90	109	82	90	103	121	70	125	130
Y	26	27	22	36	33	29	36	40	32	35	41	46	33	56	55
Sr	364	398	870	107	187	375	101	112	57	92	107	118	93	94	91
Rb	18	16	24	13	13	10	13	14	12	12	14	13	14	5	9
Th	2	2	2	2	2	n.d.	2	2	4	3	2	2	2	2	2
Pb	12	11	4	12	13	n.d.	12	12	8	10	15	12	14	n.d.	n.d.
Ga	19	17	12	17	19	n.d.	18	16	19	20	19	18	19	n.d.	n.d.
Ni	2	2	19	8	10	<	12	149	90	8	74	77	9	4	6
Co	49	43	40	46	38	n.d.	46	33	43	39	41	36	44	n.d.	n.d.
Cr	11	12	13	17	16	5	283	471	321	22	207	229	14	12	13
V	513	464	468	500	531	460	488	243	407	388	345	225	424	172	184
Ce	16	17	17	13	6	n.d.	15	11	12	18	15	24	9	n.d.	n.d.
Nd	8	9	11	6	4	n.d.	7	4	6	7	6	8	4	n.d.	n.d.
Ba	45	21	57	9	9	98	9	9	9	9	9	9	9	61	51
La	4	4	4	4	4	n.d.	4	4	4	4	4	4	4	n.d.	n.d.
Hf	6	5	5	6	6	n.d.	6	6	5	6	6	6	7	n.d.	n.d.
Sc	53	49	40	46	40	n.d.	48	39	38	41	46	33	48	n.d.	n.d.
Ti/Cr	877	744	609	543	581	1894	32	17	25	392	45	37	578	585	567
Ti/Y	371	331	360	256	282	327	250	201	255	247	227	186	245	125	134
V/Ti	0.05	0.05	0.06	0.05	0.06	0.05	0.05	0.03	0.05	0.04	0.04	0.03	0.05	0.02	0.02
Nb/Y	0.12	0.11	0.05	0.06	0.03	0.17	0.06	0.05	0.06	0.09	0.07	0.04	0.03	0.13	0.11
Zr/Ti	0.01	0.01	0.01	0.01	0.01	0.01	0.01	0.01	0.01	0.01	0.01	0.01	0.01	0.02	0.02
Zr/Y	3.65	3.44	4.05	2.61	2.52	3.21	2.50	2.73	2.56	2.57	2.51	2.63	2.12	2.23	2.36

Total Fe is expressed as FeO^*; n.d. – not determined. < – below detection limit.

textures and are dominated by plagioclase-phyric lavas. Alteration products are albite, chlorite, epidote, calcite and quartz. Basaltic andesites to andesites show intersertal, microlitic to microlitic porphyric textures. They are plagioclase-phyric, with subordinate subhedral clinopyroxene and amphibole phenocrysts. Secondary phases are mainly epidote, chlorite and calcite, indicative of greenschist facies metamorphism.

7.b. Geochemistry

A total of 41 samples of volcanic rocks were analysed for major and trace elements by X-ray fluorescence (XRF) (Table 1). The samples were collected from the basalt–radiolarite–pelagic limestone lithological association beneath the Mersin Ophiolite in the northern part of the melange (near Tavusçayırı). Major-element contents were determined on glass beads fused from ignited powders to which $Li_2B_4O_7$ was added (1:5) to a gold-platinum crucible at 1150 °C. Trace element contents were measured by XRF on pressed-powder pellets. Rare Earth Element (REE) analysis was carried out for six representative samples by the ICP-AES technique (Voldet, 1993; Table 2).

Table 2. REE contents of the volcanic rocks

	Basalt			Basaltic-andesite/Andesite		
Sample	OP-1	OP-8	OP-15	OP-9	OP-27	OP-31
La	6.80	5.20	4.50	3.90	6.00	5.90
Ce	16.10	12.90	11.30	12.40	13.80	16.90
Pr	2.30	1.80	1.80	2.10	2.10	2.60
Nd	10.50	7.90	8.10	8.80	10.60	11.90
Sm	3.10	2.60	2.50	3.20	3.50	3.60
Eu	1.15	0.96	1.15	1.18	1.33	1.40
Gd	3.90	3.10	3.80	4.30	4.90	5.00
Dy	4.70	3.70	5.50	5.60	6.50	6.90
Ho	0.93	0.77	1.05	1.06	1.34	1.38
Er	2.40	2.00	3.00	3.00	3.60	3.90
Tm	0.33	0.30	0.43	0.45	0.51	0.58
Yb	1.90	1.70	2.70	2.60	4.00	3.30
Lu	0.27	0.24	0.40	0.39	0.42	0.50

The extrusive rocks of the Mersin Melange are represented by two different lava units (Fig. 9) based on their Zr/Ti ratios and silica (SiO_2) contents (after Floyd & Winchester, 1978). The first group contains 44.09–48.17 % SiO_2, Zr/Ti ratios of 0.009–0.011 and

https://doi.org/10.1017/S0016756804009094 Published online by Cambridge University Press

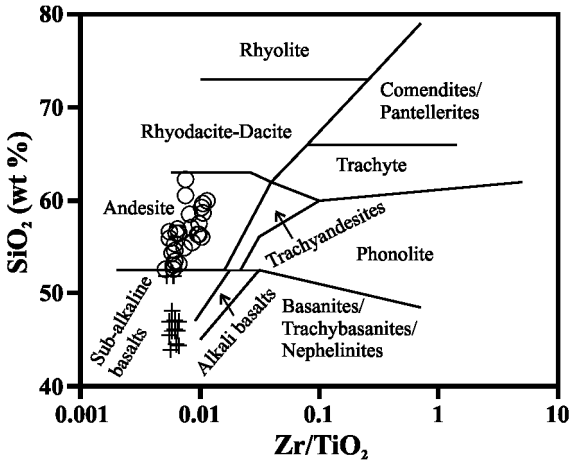

Figure 9. Discrimination of different volcanic rock types in the Mersin Melange based on SiO_2 vs. Zr/TiO_2 (after Floyd & Winchester, 1978).

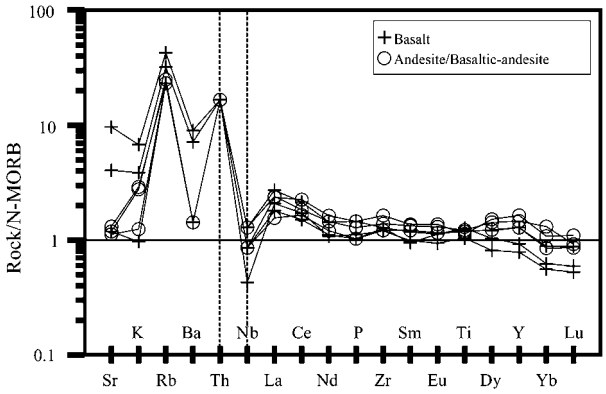

Figure 10. N-MORB normalized multi-element diagram for volcanic rocks from the Mersin Melange (normalizing values from Sun & McDonough, 1989).

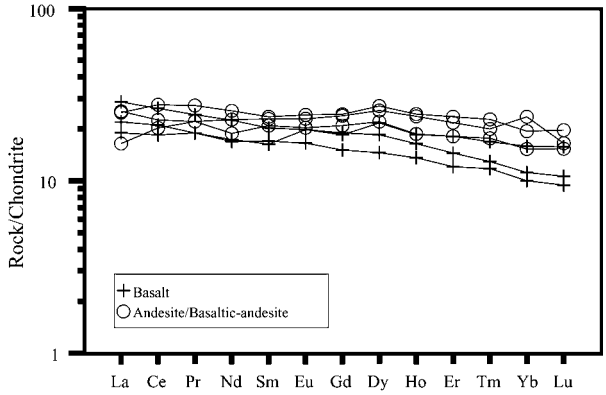

Figure 11. Chondrite-normalized REE patterns of volcanic rocks from the Mersin Melange (normalizing values from Sun & McDonough, 1989).

is classified as basalt (Fig. 9; Table 1). The second group is characterized by SiO_2 ratios of 51.95–60.58 % and Zr/Ti ratios of 0.008–0.019, and is classified as andesite. The ratios of some of the incompatible trace elements, such as Nb/Y (0.05–0.17), Zr/Y (2.91–4.05) and V/Ti (0.04–0.06), are higher in the basalts compared to andesites (Table 1).

The volcanic rocks are strongly altered, mainly due to ocean-floor hydrothermal activity, which has resulted in the loss or gain of some major and trace elements (Irvine & Baragar, 1971; Humphris & Thompson, 1978). Incompatible trace elements (e.g. Zr, Nb, Y, Ti and REE) are believed to be relatively immobile during alteration and low-grade hydrothermal metamorphism (Hart, 1970; Thompson, 1973; Pearce & Cann, 1973; Humphris & Thompson, 1978), and these elements can be used to characterize the petrological affinities and tectonic environments of eruption (Pearce & Cann, 1973; Floyd & Winchester, 1975; Pearce & Norry, 1979).

The Mersin Melange volcanic rocks exhibit: (1) low abundance of incompatible elements (e.g. Zr = 67–137 ppm, Nb = 1–7 ppm); (2) low Nb/Y ratios (0.023–0.172); (3) a wide range of Cr (1–471 ppm) and Ni (1–149 ppm) contents; (4) flat normalized REE patterns. These characteristics suggest that the volcanic rocks were derived from a depleted magma of tholeiitic character (Winchester & Floyd, 1977) (Table 1).

'Spider' plots (Fig. 10) of the basalts and andesites, when normalized against normal Mid-Ocean Ridge Basalt (N-MORB) exhibit: (1) nearly flat-lying patterns, except for Large Ion Lithophile (LIL) element enrichment (e.g. Rb, Ba, Th); (2) a marked negative Nb anomaly. Within the LIL element group, Th is relatively immobile and its enrichment relative to other incompatible elements is taken to represent the subduction zone component (Wood, Joron & Treuil, 1979; Pearce, 1982). High field strength elements (HFSE), notably Ta and Nb, are retained in the subducted slab (Perfit *et al*. 1980; Pearce, 1982; Arculus & Powel, 1986; Yogodzinski *et al*. 1993; Wallin & Metcalf, 1998), and thus a negative Nb (also Ta; not analysed) anomaly is an indication of the nature of the parental magma rather than an artefact of crystallization processes. The negative Nb anomaly (and positive Th anomaly) in the volcanic rocks analysed are interpreted to indicate a supra-subduction zone tectonic environment of eruption.

Chondrite-normalized REE patterns of the volcanic rocks within the Mersin Melange are shown in Figure 11. Total REE contents of the volcanic rocks range from 10 to 28 times chondritic values. The andesitic rocks mainly exhibit flat REE patterns ([La/Yb]N = 1.08–1.28), whereas the basaltic rocks display slightly enriched to flat REE patterns ([La/Yb]N = 1.20–2.57). These flat REE patterns are typically found in island-arc tholeiitic series (e.g. in Papua New Guinea, the Solomon Islands and Macquarie Island: Jakes & Gill, 1970), and also in supra-subduction zone-type ophiolites in Turkey, including the Mersin ophiolite (Parlak, Delaloye & Bingöl, 1997), the Pozantı–Karsantı ophiolite (Parlak,

https://doi.org/10.1017/S0016756804009094 Published online by Cambridge University Press

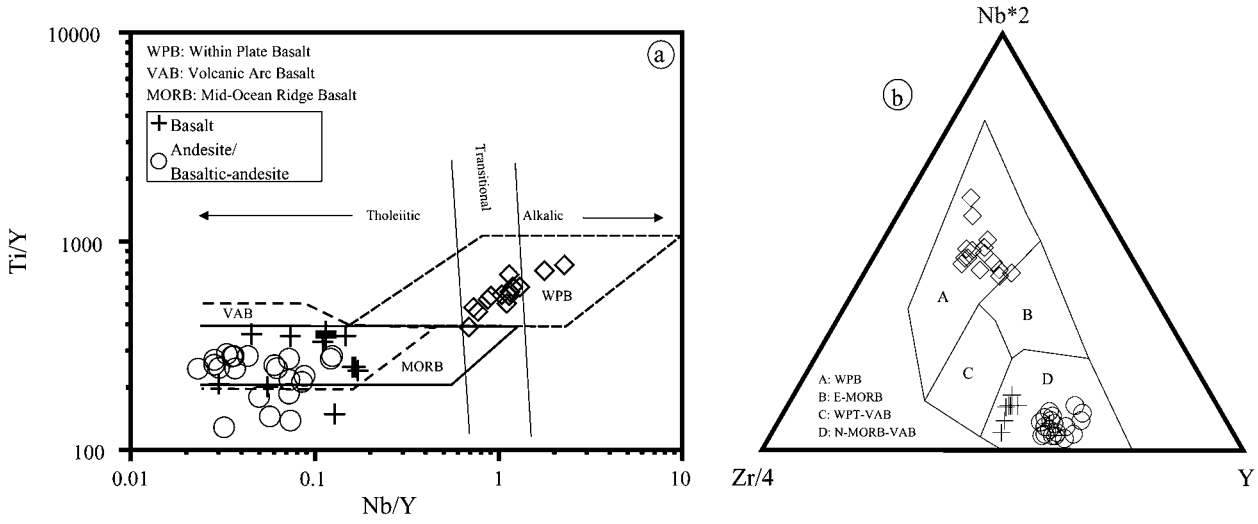

Figure 12. Geochemical discrimination diagrams of volcanic rocks from the Mersin Melange. (a) Ti/Y vs. Nb/Y (from Pearce, 1982); (b) Nb*2–Zr/4–Y (from Meschede, 1986). Metabasic rocks (diamonds) beneath the Mersin Ophiolite are also shown in both diagrams (data from Parlak, Delaloye & Bingöl, 1995).

2000; Parlak, Çelik & Delaloye, 2001; Parlak, Höck & Delaloye, 2000, 2002) and the Sarikaraman (Yaliniz, Floyd & Göncüoğlu, 1996).

The Ti/Y versus Nb/Y diagram separates within-plate basalt (WPB) from mid-ocean ridge basalt (MORB) and volcanic arc basalt (VAB) (Pearce, 1982). The analysed volcanic rocks plot in the overlapping fields of VAB and MORB (Fig. 12a). In a Zr–Nb–Y tectonomagmatic discrimination diagram (Meschede, 1986), both the basalts and andesites plot in the overlapping fields of N-MORB and VAB (Fig. 12b). The subophiolitic metamorphic rocks of the Mersin Ophiolite are also shown in both diagrams, for comparison. The metabasic rocks of the metamorphic sole, dated as Late Jurassic–Early Cretaceous in age from study of associated radiolarites, exhibit a WPB affinity in contrast to the unmetamorphosed volcanic rocks from the structurally underlying Mersin Melange. The protolith of the metamorphic sole rocks in the Mersin Ophiolite are inferred to represent seamount-type volcanic rocks of Late Jurassic–Early Cretaceous age (Parlak, Delaloye & Bingöl, 1995, 1997; Fig. 2). By contrast, the unmetamorphosed volcanic rocks of the melange are interpreted as forming by spreading above a subduction zone. They might have been accreted into the melange from the leading edge of the supra-subduction zone-type Mersin Ophiolite.

8. Granitic blocks within the melange

8.a. Field relations and petrography

Granitic rocks occur locally, south of Tavusçayırı Tepe (Fig. 4), as blocks and lenses within serpentinized harzburgite, gabbro and highly altered basaltic rocks (Fig. 4). The largest body, a few tens of metres across, is aligned along a NE–SW-trending tectonic lineament. Lithologies are generally meta-granite and meta-microgranite and show granular, microgranular and poikilitic textures. These rocks are characterized by anhedral quartz (35–45 %), alkali feldspar (35 %), plagioclase (10 %) and muscovite (10 %), with minor amounts of biotite (1–5 %) and garnet (1–5 %). Kaolinization, sericitization and chloritization are extensively developed.

The main granitic body was strongly deformed during incorporation into the melange. The granitic rocks were metamorphosed to garnet–mica schist. Microprobe analysis (Table 3) shows that the garnets are dominated by an almandine (> 80 %) end-member and have average core and rim compositions of Al78, Py7, Sp10, And5 and Al82, Py7, Sp7, And4, respectively. Miller & Stoddard (1981) pointed out that most garnets in granitic rocks are rich in Mn relative to Fe–Mg and contain a spessartine component exceeding 10 mol. %. The garnets in our samples have a spessartine component ranging from 4–12 mol. % and are, therefore, likely to be of metamorphic origin. Almandines formed during regional metamorphism commonly show a zoning marked by Mn-rich cores and Fe-rich margins (Deer, Howie & Zussman, 1992), as seen in this case (Table 3).

8.b. Geochemistry and origin

Major and trace element analysis was carried out on 12 granite samples using the XRF method (specified earlier) for the volcanic rocks. In addition, two granite samples were analysed for REE concentrations by ICP-AES (Voldet, 1993).

Major, trace and REE analyses of granitic rocks are given in Table 4. The granitic rocks exhibit high

https://doi.org/10.1017/S0016756804009094 Published online by Cambridge University Press

Table 3. Representative microprobe analysis of the garnets from the metagranites within the Mersin Melange

Sample	271-2c	271-2r	271-3c	271-3r	271-5c	271-5r	148-1c	148-1r	148-3c	148-3r	148-4c	148-4r
SiO_2	36.53	36.43	36.54	36.66	36.37	36.68	36.66	36.67	36.57	36.80	36.62	36.55
TiO_2	0.00	0.01	0.03	0.00	0.01	0.00	0.03	0.00	0.02	0.02	0.05	0.04
Al_2O_3	20.93	20.76	20.86	20.71	20.65	20.91	20.96	20.82	20.71	20.82	20.91	20.72
Cr_2O_3	0.00	0.02	0.00	0.04	0.00	0.00	0.00	0.00	0.00	0.00	0.00	0.02
FeO	37.48	38.09	37.50	38.00	35.02	37.63	35.99	36.93	35.60	37.01	34.62	35.24
MnO	2.28	1.89	2.63	1.88	4.07	2.02	3.68	3.44	4.40	3.64	5.19	4.47
MgO	1.89	1.86	1.88	1.91	1.57	1.87	1.81	1.75	1.76	1.81	1.65	1.79
CaO	1.32	1.16	1.39	1.18	1.70	1.22	1.58	1.20	1.58	1.21	1.49	1.40
Total	100.43	100.22	100.83	100.38	99.95	100.33	100.71	100.81	100.64	101.31	100.53	100.23
Si	5.92	5.92	5.90	5.95	5.74	5.95	5.93	5.93	5.92	5.92	5.94	5.94
Ti	0.00	0.00	0.00	0.00	0.00	0.00	0.00	0.00	0.00	0.00	0.01	0.00
Al IV	0.08	0.08	0.10	0.05	0.26	0.05	0.07	0.07	0.08	0.08	0.06	0.06
Al VI	3.92	3.90	3.88	3.91	3.58	3.95	3.92	3.90	3.87	3.88	3.93	3.91
Cr	0.00	0.00	0.00	0.01	0.00	0.00	0.00	0.00	0.00	0.00	0.00	0.00
Fe^{3+}	0.16	0.17	0.21	0.13	1.26	0.10	0.15	0.16	0.20	0.19	0.12	0.14
Fe^{2+}	4.92	5.01	4.85	5.02	3.36	5.01	4.72	4.83	4.62	4.79	4.57	4.65
Mn	0.31	0.26	0.36	0.26	0.54	0.28	0.50	0.47	0.60	0.50	0.71	0.62
Mg	0.46	0.45	0.45	0.46	0.37	0.45	0.44	0.42	0.42	0.43	0.40	0.43
Ca	0.23	0.20	0.24	0.21	0.29	0.21	0.27	0.21	0.27	0.21	0.26	0.24
End-member												
Almandine	83.13	84.59	82.17	84.44	73.68	84.17	79.53	81.43	78.02	80.78	76.94	78.26
Pyrope	7.71	7.61	7.67	7.77	8.10	7.60	7.36	7.11	7.17	7.33	6.71	7.30
Spessartine	5.29	4.39	6.09	4.34	11.92	4.66	8.50	7.94	10.19	8.37	11.99	10.35
Andradite	3.87	4.11	5.19	3.28	6.02	2.37	3.65	4.05	4.88	4.79	2.97	3.38

Numbers of ions on the basis of 24 (O); c and r indicate core and rim, respectively.

Table 4. Representative major, trace and rare earth element analyses of the granites

Sample	OP-148a	OP-148b	OP-262	OP-264	OP-268	OP-269	OP-272	OP-324	OP-337
SiO_2	77.29	74.72	74.77	75.27	74.5	76.02	75.36	77.53	77.34
Al_2O_3	13.75	14.95	14.55	13.41	14.47	14.02	13.96	12.21	12.38
TiO_2	0.17	0.20	0.21	0.26	0.23	0.17	0.16	0.14	0.09
FeO^*	1.79	1.99	2.00	2.64	2.17	1.65	1.45	1.36	1.26
CaO	0.84	1.34	1.32	1.07	1.48	1.33	1.32	2.22	1.67
MgO	0.63	0.50	0.47	0.67	0.51	0.37	0.39	0.37	0.23
Na_2O	2.87	4.53	3.64	3.65	3.94	3.52	3.62	4.47	5.82
K_2O	1.85	1.28	1.64	1.96	1.53	1.60	1.53	0.50	0.28
MnO	0.06	0.02	0.03	0.04	0.03	0.02	0.01	0.02	0.02
P_2O_5	0.03	0.11	0.08	0.07	0.10	0.10	0.10	0.02	0.02
LOI	1.20	0.97	1.18	1.16	1.09	1.08	1.07	0.75	0.71
Total	98.98	100.59	99.88	100.19	100.05	99.87	98.96	99.58	99.81
Ba	619	273	632	663	533	622	562	145	168
Ni	6	7	6	16	5	13	38	21	38
V	28	30	25	34	26	21	17	18	12
Cr	16	52	29	32	21	15	22	25	26
Nb	4	9	8	6	8	9	12	4	4
Zr	92	89	90	161	87	87	89	180	89
Y	20	34	34	33	32	29	29	17	30
Sr	164	274	169	182	176	170	180	98	56
Rb	90	72	86	117	82	86	86	28	19
La	10.2	15.8							
Ce	21.7	31.8							
Pr	2.8	4.1							
Nd	11	15.4							
Sm	2.8	3.7							
Eu	0.74	1.26							
Gd	2.6	3							
Dy	3.3	3.7							
Ho	0.72	0.82							
Er	2	2.4							
Tm	n.d	0.38							
Yb	1.9	2.3							
Lu	0.27	0.34							

Total Fe is expressed as FeO^*. n.d. – not determined.

https://doi.org/10.1017/S0016756804009094 Published online by Cambridge University Press

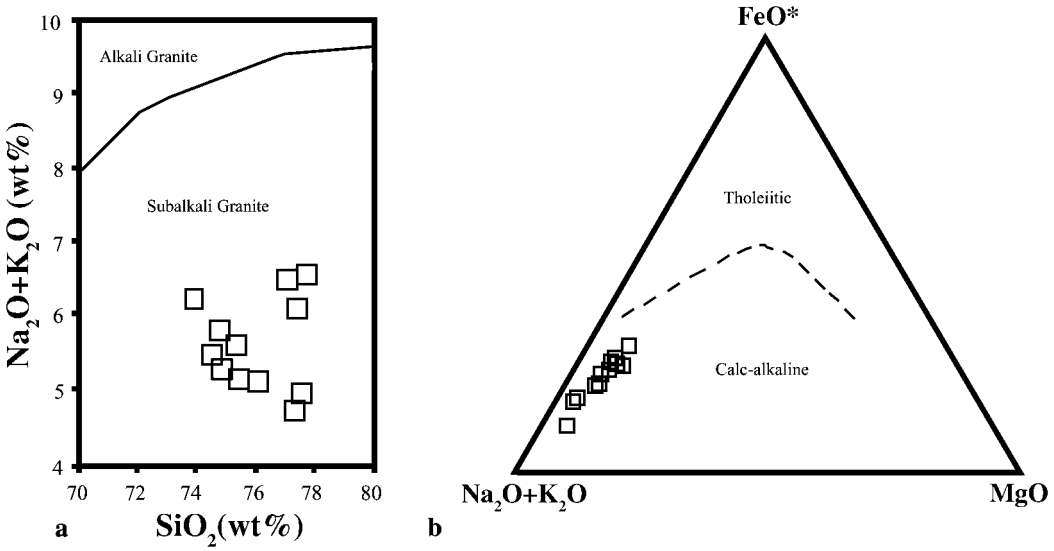

Figure 13. (a) Na_2O+K_2O vs. SiO_2 variation diagram (after Cox, Bell & Pankhurst, 1979). The dividing line between alkali and subalkali granitoid is from Miyashiro (1978). (b) AFM diagram for the granitic rocks in the study area (after Irvin & Baragar, 1971).

SiO_2 (74–77 %), Na_2O (3–6 %), K_2O (0.3–2 %), Al_2O_3 (12–15 %) and MgO (0.3–0.7 %). The major element concentrations are thus strongly altered. Trace element concentrations are also variable, particularly Nb (2–12 ppm), Y (17–34 ppm), Zr (87–180 ppm) and Rb (26–117 ppm).

Geochemical evidence for the tectonic setting of the granitic rocks relies on major–trace element discrimination diagrams (Pearce, Harris & Tindle, 1984; Harris, Pearce & Tindle, 1986). The granitic rocks studied plot in the subalkali granite field based on the SiO_2 versus Na_2O+K_2O plot of Cox, Bell & Pankhurst (1979) (Fig. 13a); they show a calc-alkaline affinity in the AFM diagram of Irvine & Baragar (1971) (Fig. 13b). Granitic rocks showing a calc-alkaline tendency are widely interpreted as the products of volcanic arc magmatism (Peacock, 1931; Shand, 1951). In the tectonic discrimination diagrams based on immobile trace elements, the granitic rocks in the ophiolitic melange plot on the Volcanic Arc Granite–Syncollisional Granite field (VAG–SynCOLG) in the Nb–Y ternary diagram (Pearce, Harris & Tindle, 1984; Fig. 14a). The granitic rocks plot in the Volcanic Arc Granite field (VAG) using the Rb versus Y + Nb diagram (Pearce, Harris & Tindle, 1984; Fig. 14b) and on the Rb/Zr versus SiO_2 plot (Harris, Pearce & Tindle, 1986; Fig. 14c). The REE pattern is shown in Figure 15a. The granites exhibit high LREE/HREE ratios and moderate REE contents ranging from 60 to 85 ppm. Eu/Sm ratios are between 0.26 and 0.34 and weak Eu anomalies are present. The overall REE abundances may indicate little or no residual plagioclase in the source (Cullers & Graf, 1984). The REE pattern of the granitic rocks is suggestive of VAG origin. Ocean-ridge granite (ORG)-normalized trace element patterns of the granitic rocks show LIL (K_2O, Rb, Ba) and Ce and Sm enrichment relative to Nb, Zr, Y. Large ion lithophile (LIL) elements are 2 or 20 times higher than the ORG (ocean ridge granite), whereas HFS elements are less than ORG. These patterns resemble the trace element patterns commonly seen in volcanic arc granites (Pearce, Harris & Tindle, 1984; Fig. 15b).

8.c. Geochronology

Five muscovite separates were used for K–Ar analysis of granite in order to shed light on the time of intrusion. The K content of each sample was measured by Atomic Absorption Spectrometry. Ar was extracted by total sample fusion into a pyrex line fitted with high vacuum metal valves. The resultant gas was mixed with a ^{38}Ar spike to apply the isotopic dilution technique. Contaminating gases were separated with titanium traps and liquid nitrogen. Measurements were done in static mode with an AEI MS-10S spectrometer fitted with a permanent magnet of 4.1 kG and connected to a computer for processing data. Samples were degassed at about 100 °C for several hours before the analysis to reduce atmospheric contamination. Analytical precision is near 0.5 %. The constants of Steiger & Jäger (1977) were used to calculate an age.

The calculated cooling ages (Table 5) range widely from 332.6 ± 6.5 Ma (Early Carboniferous) to 390.8 ± 7.5 Ma (Early–Mid-Devonian). The overall isochron age is 375.7 ± 10.5 Ma (Late Devonian). Assuming the meta-granite represents a co-magmatic/cogenetic group, it is possible that the disparate calculated ages resulted from metamorphism of magmatic muscovite.

8.d. Interpretation: significance of Devonian granite

We think it likely that the meta-granite represents a fragment of Palaeozoic 'basement rocks', which

https://doi.org/10.1017/S0016756804009094 Published online by Cambridge University Press

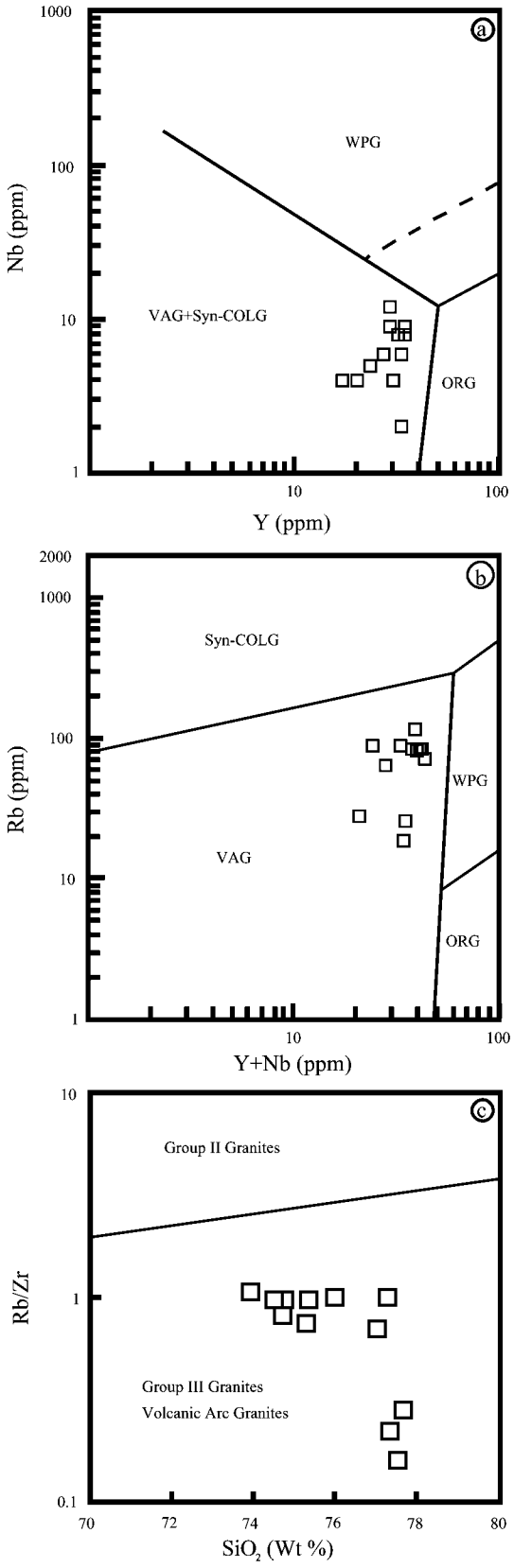

Figure 14. (a) Nb vs. Y (after Pearce, Harris & Tindle, 1984); (b) Rb vs. Y + Nb (Pearce, Harris & Tindle, 1984); (c) SiO_2 vs. Rb/Zr (after Harris, Pearce & Tindle, 1986) diagrams for the granites in the Mersin Melange. VAG – Volcanic arc granite; SynCOLG – Syncollisional granite; ORG – Ocean-ridge granite; WPG – Within-plate granite.

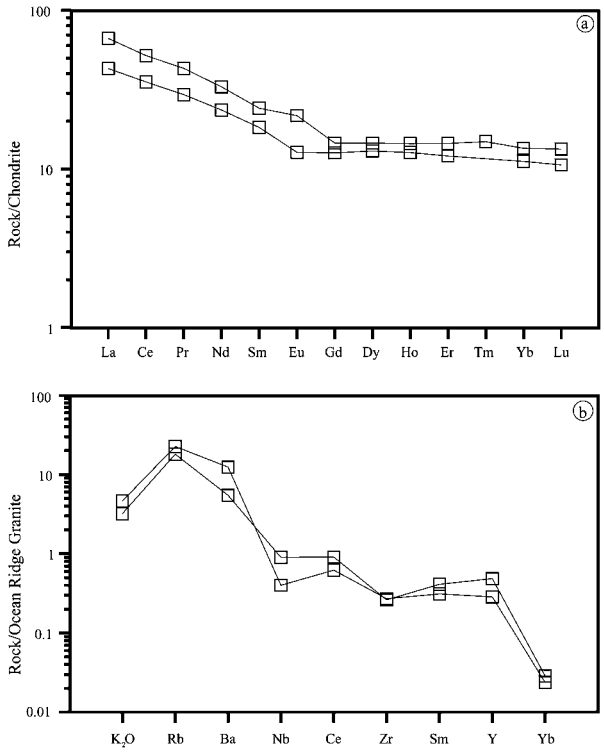

Figure 15. (a) Chondrite-normalized REE patterns (normalizing values are from Sun & McDonough, 1989) and (b) ocean-ridge granite (ORG)-normalized multi-element diagram (normalizing values from Pearce, Harris & Tindle, 1984) for the granites in the Mersin Melange.

became incorporated into the Mersin Melange during its Late Cretaceous emplacement. Comparable granitic rocks are not known in other allochthonous Mesozoic units bordering the Tauride Carbonate Platform. A possible source of the meta-granites in the Mersin Melange could be from the unexposed northern margin of the Tauride Carbonate Platform. The Late Palaeozoic granitic rocks relate to southward subduction beneath the Bolkar Dağ, assuming this was then part of the northern margin of Gondwana (Göncüoğlu & Kozlu, 2000).

Alternatively, the palaeotectonic maps of Stampfli *et al*. (2001) suggest that the granites might have formed along the southern margin of Eurasia in response to northward subduction. They were later emplaced onto the southerly (Gondwana) margin in response to closure of an intervening Tethyan ocean by latest Triassic time. Once emplaced onto the southerly (Gondwana) margin, the granites became part of the Tauride microcontinent and were finally emplaced as part of the Mersin Melange in latest Cretaceous time. However, it is difficult to reconcile this scenario (that is, an Eurasian margin origin of the meta-granite) with the inferred tectonic history of the northern margin of the Tauride Carbonate Platform, which is interpreted in terms of Triassic rifting (Monod, 1977; Özgül, 1984, 1997; Andrew & Robertson, 2002) rather than closure and collision.

https://doi.org/10.1017/S0016756804009094 Published online by Cambridge University Press

Table 5. K-Ar ages and analytical data for the granites in the Mersin Melange

Sample	Material	%K	$^{40}Ar^{*}$ moles/g $\times 10^{-11}$	$\%^{40}Ar^{*}$	$^{40}Ar/^{36}Ar$ ($\times 10^{2}$)	$^{40}K/^{36}Ar$ ($\times 10^{4}$)	Age (Ma)
OP-262	Muscovite	7.5	474.999	98.3	171.51	79.43	332.6 ± 6.5
OP-268	Muscovite	6.7	503.908	97.4	112.18	43.08	390.8 ± 7.5
OP-269	Muscovite	7.5	508.627	98.7	229.41	99.66	354.0 ± 6.9
OP-271	Muscovite	7.5	515.796	97.6	121.04	51.25	358.5 ± 6.9
OP-272	Muscovite	6.8	486.826	93.5	45.15	17.67	370.3 ± 7.1

The geochemical data (Fig. 13a) suggest that the meta-granites are likely to be subduction related. However, in the absence of more diagnostic isotopic data, it is also possible that the subduction signature was inherited from one or more older pre-existing subduction events in the area. For example, Panafrican granites are known to occur within the Menderes Massif further west (e.g. Kröner & Şengör, 1990). Such rocks could have influenced the geochemical signature of any younger magmatic rocks in the area.

9. Structure of the metamorphic sole

The structure of the metamorphic sole of the Mersin Ophiolite is relevant here as it was reported to provide kinematic evidence for northward emplacement of the ophiolite in latest Cretaceous time (Parlak, Bozkurt & Delaloye, 1996).

The ophiolitic sole is exposed at only a few localities beneath the ophiolite (Parlak, Delaloye & Bingöl, 1995; Parlak, Bozkurt & Delaloye, 1996; Fig. 2). The main lithology of the metamorphic sole is amphibolite, with subordinate greenschist, marble and meta-chert. These metamorphic rocks are located between the harzburgite tectonites of the ophiolite and the melange below. The metamorphic sole exhibits a classic inverted metamorphic gradient, from amphibolite facies metamorphic rocks, downward into greenschist facies rocks and then into unmetamorphosed melange. Geochemical studies show that the protoliths of the meta-igneous rocks are basalts of within-plate type (WPB) and were interpreted as emplaced remnants of oceanic seamounts (Parlak, Delaloye & Bingöl, 1995). The protoliths are envisaged as being accreted to the base of the still-hot ophiolite, related to intra-oceanic detachment and subduction (Parlak, Bozkurt & Delaloye, 1996).

The metamorphic sole is cut by unmetamorphosed diabase/micrograbbro dykes that display an island-arc tholeiite (IAT) character (Parlak & Delaloye, 1996). These dykes may relate to the initial stages of oceanic arc-type magmatism and were intruded prior to emplacement of the ophiolite and melange onto the Tauride Carbonate Platform. ^{40}Ar–^{39}Ar dating of hornblende separates from the metamorphic sole yielded an age of 92.6 ± 0.2 Ma, interpreted as the time of initial detachment of oceanic crust during closure of Neotethys (Parlak & Delaloye, 1999).

During this study, we focused on trying to obtain kinematic evidence for the early stages of emplacement of the metamorphic sole (prior to diabase dyke intrusion) while still in an oceanic setting. We measured the orientations of a well-developed stretching lineation within amphibolites at three main localities (Fig. 16a–c). Other aspects of the structure of these localities were previously described by Parlak, Bozkurt & Delaloye (1996). Taken together, the trend of the early ductile stretching lineation varies from NE–SW to SE–NW and plunges mainly at moderate angles. The average trend is nearly E–W. The stretching lineation is associated with the formation of early ductile, high-temperature-type folds. The axial planes of these ductile folds generally parallel the stretching lineation. Locally, the folds verge mainly northwards, which was previously taken to indicate a northward tectonic transport direction (Parlak, Bozkurt & Delaloye, 1996). However, fold vergence is not a reliable indicator of tectonic transport direction under high-temperature ductile conditions (under which transport lineations parallel fold axial planes). On the other hand, the later stages of brittle deformation affecting the metamorphic sole, the base of the ophiolite and the post-metamorphic diabase dykes are mainly northward directed, in agreement with Parlak, Bozkurt & Delaloye (1996).

We conclude that that the ophiolite and sole underwent generally E–W or W–E tectonic transport with respect to present geographic coordinates. However, these coordinates could have changed as a result of intra-oceanic rotation about a high angle (e.g. Morris *et al*. 2002). The metamorphic sole, therefore, provides no direct evidence for the initial direction of the movement of the ophiolite while still in an oceanic setting.

10. Restoration of the Mersin Melange

The four lithological associations recognized within the Mersin Melange (Fig. 6) are (1) the Upper Permian–Upper Cretaceous shallow-water carbonate association; (2) the Upper Triassic–Upper Cretaceous volcanic–terrigenous–pelagic association; (3) the Upper Jurassic–Upper Cretaceous basalt–radiolarite pelagic limestone association and (4) the Upper Cretaceous ophiolite-derived association. Each of these lithological associations varies from broken formation to melange and is associated with a matrix of both sedimentary and tectonic origin.

https://doi.org/10.1017/S0016756804009094 Published online by Cambridge University Press

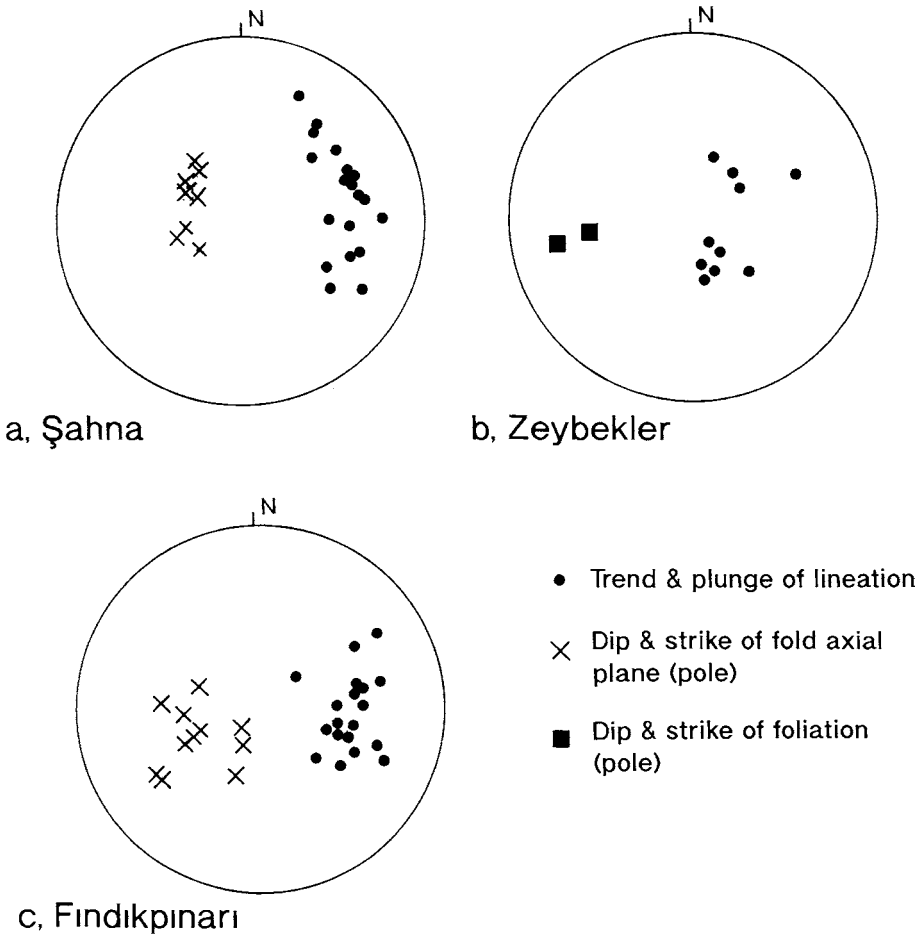

Figure 16. Stereographic projections (Equal area, Lower Hemisphere) of structural data from early ductile fabrics in the metamorphic sole of the Mersin Ophiolite. See text for explanation. (a) Data from amphibolites exposed in the stream below Şahna village; (b) road section, 2 km N of Zeybekler village (between Fındıkpınarı and Şahna); (c) road section between Fındıkpınarı and Tepeköy villages (5 km N of Fındıkpınarı).

The shallow-water carbonate association (1) is interpreted as a rifted carbonate platform that finally underwent submergence in Late Cretaceous time. The volcanic–terrigenous–pelagic association (2) is presents a volcanically active Triassic rift, overlain by Upper Triassic–Upper Cretaceous pelagic sediments, including a Late Jurassic–Early Cretaceous siliceous interval. The basalt–chert–pelagic limestone association (3) comprises oceanic basalts of supra-subduction zone-type chemical affinities, associated with siliceous (radiolarian) and calcareous pelagic sediments. Where present, the sedimentary melange matrix records gravity reworking in a deep-marine basinal setting, contemporaneous with melange emplacement during Late Cretaceous time.

An obvious restoration is to order lithological associations 1–4 from proximal carbonate platform, to rifted margin, to oceanic. The over-riding Mersin Ophiolite is inferred to have formed in a supra-subduction zone setting (Parlak, Delaloye & Bingöl, 1996, 1997). The Late Triassic intervals of the carbonate–radiolarite–pelagic carbonate succession vary considerably from shallow-water, to submerged shelf, to unstable slope successions and basinal assemblages. This implies the existence of a varied horst-graben seafloor topography during and after rift volcanism. Many of the smaller limestone blocks throughout the melange are composed of slope facies (e.g. calciturbidites and gravity deposited breccias) suggesting that platform margin units were strongly fragmented and mixed with the melange during its formation.

11. Evidence from the Tauride Carbonate Platform and further north

A key question is the location of the root zone of the Mersin Melange, either to the north or to the south of the E–W-trending Tauride Carbonate Platform (Fig. 2). Structural evidence from the melange, metamorphic sole and the ophiolite provide some indications of northward displacement under conditions of brittle deformation, but provide no direct evidence for the sense of initial movement of the ophiolite and metamorphic sole within the ocean under high-temperature ductile conditions. However, there is indirect support for

https://doi.org/10.1017/S0016756804009094 Published online by Cambridge University Press

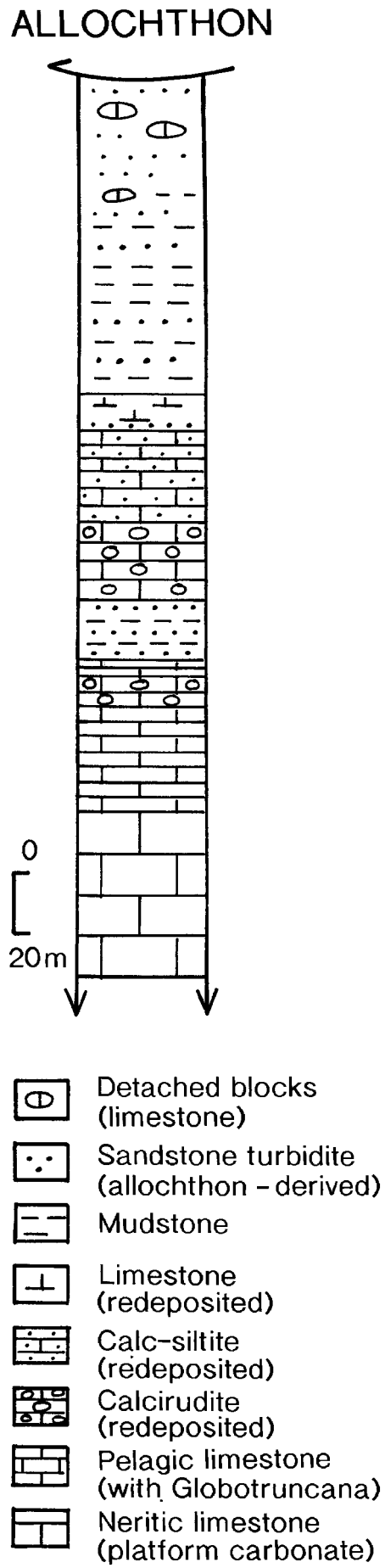

southward emplacement from a comparison, both with relatively autochthonous Mesozoic Tauride Carbonate Platform successions to the north and with ophiolitic and melange units exposed further northwest.

North of the Mersin Melange, the Bolkar Dağ (correlated with the Tauride Carbonate Platform), is divided into two major thrust sheets, known as the Southern and Northern Bolkar Dağ units (Fig. 2). In the Southern Bolkar Dağ (Fig. 6), Upper Permian shallow-water carbonates (*c*. 600 m thick Öşün Formation), pass into Triassic limestones, sandstones and shales with detached blocks of Permian limestone (*c*. 600 m thick Kargedik Formation). These lithologies are unconformably overlain by shallow-water carbonates (limestones and dolomites), several kilometres thick, of Early Jurassic to Late Cretaceous age (Cehennemdere Formation). The succession passes transitionally upwards into siliceous pelagic limestones and then into lithoclastic turbidites and debris-flow deposits containing ophiolite-derived material and detached blocks of Permian, Triassic and Jurassic limestone (several hundred metre-thick Aslanköy Formation). Interbedded pelagic and hemi-pelagic carbonates contain planktic foraminifera of Late Cretaceous age (Demirtaşlı *et al*. 1984).

During this study we logged a succession (near Yavça; Fig. 17). This records initial destabilization of the drowned carbonate platform, followed by input of sediment both from the collapsing carbonate platform (mainly as calciturbidites and debris-flow deposits) and from the advancing allochthon (as lithoclastic muds and sand/silt turbidites). Deposition culminated in a mudstone/sandstone turbidite succession mainly derived from the advancing allochthon, with the addition of detached blocks (olistoliths) derived from the Bolkar Dağ platform. This succession is interpreted to record collapse of the carbonate platform related to flexure and loading related to an allochthon advancing from the Northern Neotethys.

The Northern Bolkar Dağ succession (Fig. 6) is similar to the Southern Bolkar Dağ succession, but is generally more metamorphosed to marble, with slate and schist intercalations especially in the north. Permian neritic carbonates, with local bauxite lenses, are overlain by Lower–Middle Triassic shallow-marine shales and impure carbonates. Diabase sills are present in the north. Thick shallow-water platform carbonates of Late Triassic age, with minor bauxite, form the highest mountains (up to 3524 m). Shallow-water carbonates of Jurassic–Late Cretaceous age follow,

Figure 17. Measured sedimentary log of the Late Cretaceous sedimentary transition from the top of the intact Tauride Carbonate Platform to the overlying allochthon (S Bolkar Dağ unit, near Yavça). The intervening sediments record the collapse of the platform and deposition of clastic sediment derived from the advancing allochthon.

https://doi.org/10.1017/S0016756804009094 Published online by Cambridge University Press

again with bauxite layers. There is a transition to deeper marine pelagic carbonates at the top of the succession.

The Northern Bolkar Dağ unit is thrust northwards over ophiolitic melange and a dismembered ophiolite, known locally as the Alihoca ophiolite (Dilek & Whitney, 1997); Clark & Robertson, 2002). This forms part of the larger Pozantı–Karsantı ophiolite which extends further east onto the Aladağ (Çakır, 1978; Juteau, 1980; Tekeli *et al*. 1984; U. Ünlügenç, unpub. Ph.D. thesis, Keele Univ, 1993; Lytwyn & Casey, 1995; Polat, Casey & Kerrich, 1996; Fig. 1). Several isolated ophiolite klippen tectonically overlie the meta-platform carbonate succession in the eastern part of the Northern Bolkar Dağ unit. One of these, the Kiziltepe ophiolitic thrust sheet, consists of serpentinized peridotite and metamorphosed extrusive rocks, and is tectonically underlain by a thin sliver of foliated amphibolites. In the Northern Bolkar Dağ unit, these amphibolitic rocks exhibit a HP/LT (high pressure/low temperature) blueschist facies overprint (Dilek & Whitney, 1997).

Both of the local Bolkar Dağ unit successions record Late Permian shallow-water carbonate deposition, followed by Early–Mid-Triassic rifting, associated with basic magmatism exposed in the north. This was followed by passive subsidence during Late Triassic–Late Cretaceous time. During the Late Cretaceous, ophiolite-derived sediments and detached ophiolite blocks were shed into a foredeep, derived from continental margin and ophiolite units. These units were emplaced southwards onto the Bolkar Dağ unit regionally, as shown by kinematic evidence (Polat & Casey, 1995). Shallow-marine transgression occurred as early as Maastrichtian time along the northern margin of the Northern Bolkar Dağ unit (Demirtaşlı *et al*. 1984; Clark & Robertson, 2002). The area to the southwest of the Northern Bolkar Dağ unit includes inliers of post-emplacement ophiolite-derived conglomerates that are dated as Early Paleocene (Demirtaşlı *et al*. 1984), suggesting that the emplacement of the allochthonous rocks was completed soon after latest Cretaceous time.

The evidence from the Bolkar Dağ carbonate platform to the north of the Mersin Melange, therefore, indicates that the platform collapsed and was overridden by allochthonous ophiolitic rocks in latest Cretaceous time but does not prove the direction of emplacement.

12. Regional comparisons

To shed further light on the question of emplacement direction, the Mersin Melange can be compared with other melange units exposed generally to the north and south of the Tauride Carbonate Platform (Fig. 1). The Tauride Carbonate Platform is widely reconstructed as a microcontinent within the Mesozoic Tethyan ocean (Neotethys: Şengör & Yılmaz, 1981; Robertson & Dixon, 1984; Dercourt, Ricou & Vrielynck, 1993). Relevant units to the north are the Beyşehir–Hoyran–Hadim Nappes, which extend for > 500 km E–W along the northern margin of the Tauride Carbonate Platform to the northwest of the Mersin Melange exposures. There are also to the south the Baer–Bassit ophiolite (northern Syria), the Mamonia Complex (western Cyprus) and the Antalya Complex (southwestern Turkey). These northerly and southerly units are restored to original locations within the northern and southern Neotethys, respectively (Robertson & Woodcock, 1982; Şengör & Yılmaz, 1981; Robertson *et al*. 1991; Robertson, 1998, 2000).

12.a. Northerly derived units: the Beyşehir–Hoyran Nappes

The Mersin Melange exhibits many similarities with the Beyşehir–Hoyran Nappes that structurally overlie the northern margin of the Tauride Carbonate Platform: (1) Each of the four lithological associations of the Mersin Melange can be correlated with a thrust sheet within the Beyşehir–Hoyran Nappes as a whole. (2) Upper Permian shallow-water carbonates are locally present in both areas, although restricted to occasional blocks within the melange in the Beyşehir–Hoyran Nappes (Beyşehir area; Monod, 1977). Triassic–Cretaceous shallow-water carbonates (Gencek-type units) are important in both areas. (3) Triassic–Cretaceous terrigenous–volcanogenic–neritic–pelagic units (Huğlu-type units) form another major succession in both areas. (4) In the Beyşehir–Hoyran Nappes, Ammonitoco Rosso of Toarcian age (Monod, 1977) is overlain by red ribbon radiolarites, then by Upper Cretaceous pelagic carbonates. A similar succession including Ammonitoco Rosso occurs in the Mersin Melange. (5) Late Cretaceous debris-flow deposits, similar to those of the Mersin Melange, form a matrix to some units of the Beyşehir–Hoyran Nappe (the 'Wildfysch' of Monod, 1977, or the syn-tectonic debris flows of Andrew & Robertson, 2002).

The nearest exposures of the Beyşehir–Hoyran Nappes to the Mersin Melange are located in the Karaman area, *c*. 100 km to the northwest (the Insaniye and Oğuklu Dağ units: Andrew & Robertson, 2002; T. Andrew, unpub. Ph.D. thesis. Univ. Edinburgh, 2003; Fig. 1). Logged successions from this area of the Beyşehir–Hoyran Nappes are similar to those of the Mersin Melange, including the presence of siliceous tuff, nodular carbonates and radiolarites in both areas (Fig. 7).

The main difference between the Beyşehir–Hoyran Nappes and the Mersin Melange is the structural style, as follows. (1) The Beyşehir–Hoyran Nappes include relatively coherent stratigraphic successions, in contrast to the melange and broken formation

https://doi.org/10.1017/S0016756804009094 Published online by Cambridge University Press

of the Mersin Melange. Despite this, in some areas the Beyşehir–Hoyran Nappes are strongly tectonically disrupted, creating broken formation and melange (Andrew & Robertson, 2002) similar to the Mersin Melange. (2) The large-scale thrust stacking order differs in the two areas. In the Mersin Melange the ophiolite occurs at the top of the thrust stack, followed (downwards) by the metamorphic sole and then by the Mersin Melange. By contrast, in the Beyşehir–Hoyran Nappes the ophiolite and related melange (e.g. in the Beyşehir area) occurs near the base of the thrust stack with, above it, a volcanic-sedimentary (Huğlu-type) units, a neritic unit (Gencek-type units) and a neritic–pelagic (Boyalı Tepe-type) unit. There is some local variation in the relative order of these upper volcanic–sedimentary thrust sheets but all overlie the ophiolite (Andrew & Robertson, 2002).

The unusual stacking order of the Hoyran–Beyşehir Nappes was explained by southward re-thrusting during Late Eocene time (Andrew & Robertson, 2002). During this event, part of the northern margin of the Tauride Carbonate Platform was detached and thrust southwards forming the regionally extensive Hadim Nappe (that includes Palaeozoic–Lower Tertiary successions), with the Hoyran–Beyşehir Nappes riding above. During the inferred re-thrusting the ophiolite was relocated near the base of the Hoyran–Beyşehir Nappes. The Hadim Nappe and associated effects of rethrusting are not known to extend as far east as the Mersin Melange (Özgül, 1984; Demirtaşlı *et al*. 1984). In this easterly region both the northern margin (Demirtaşlı *et al*. 1984; Clark & Robertson, 2002) and the southern margin (Avşar, 1992) of the Bolkar Dağ carbonate platform are unconformably overlain by undeformed Maastrichtian to Early Tertiary transgressive units. The northern margin of the Bolkar Dağ was affected by thrusting and folding in Late Eocene time (Clark & Robertson, 2002), but there is no evidence of Late Eocene compression affecting the Mersin Melange further south. Prior to Late Eocene re-thrusting it is, therefore, likely that the tectonostratigraphy of the Mersin Melange and the Beyşehir–Hoyran Nappes were very similar and that they formed contiguous units along the northern margin of the Tauride continental unit.

Structural evidence (Andrew & Robertson, 2002) shows that the Hoyran–Beyşehir Nappes were initially emplaced southwards onto the Tauride Carbonate Platform in latest Cretaceous time (Monod, 1977; Özgül, 1984), and thus must be restored to a position along the northern margin of the Tauride Carbonate Platform. The volcanogenic–terrigenous–pelagic (Huğlu-type) units are interpreted as a marginal rift and the Triassic neritic carbonates (Gencek-type units) as a marginal part of the Tauride Carbonate Platform. Triassic neritic carbonates overlain by Toarcian Ammonitoco Rosso (Boyalı Tepe-type units) are interpreted as submerged off-margin carbonate highs. These restored settings of the Hoyran–Beyşehir Nappes are consistent with our interpretation of the Mersin Melange.

12.b. Southerly derived units

In northern Syria, the Baer–Bassit Melange structurally underlies, and is interleaved with, the Late Cretaceous Baer–Bassit ophiolite (Delaune-Mayère, 1984; Parrot, 1977; Whitechurch, 1977; Delaloye & Wagner, 1984; Al-Riyami & Robertson, 2002). Some features are comparable with the Mersin Melange: (1) the melange is intergradational between severely disrupted thrust sheets, broken formation and melange; (2) a metamorphic sole and a complete (but dismembered) ophiolite are present; (3) the protoliths of the metamorphic sole rocks are within-plate type alkaline basalt (inferred seamounts).

However, there are many differences: (1) no lithologies older than Late Triassic carbonates are known in Baer–Bassit; (2) Late Triassic rift-related, mixed volcanic–terrigenous successions are absent; (3) Triassic–Cretaceous shelf carbonates are absent; only slope to basinal facies are preserved; (4) the matrix of the Baer–Bassit melange is almost entirely tectonic in origin, with minimal syn-emplacement sediments (Al-Riyami & Robertson, 2002). The Baer–Bassit Melange is interpreted as part of the northern margin of the southern Neotethys, that is, related to the Arabian margin (Al-Riyami & Robertson, 2002).

Similarities with the Mamonia Complex of southwestern and western Cyprus are restricted to a Late Triassic to Cretaceous age and the presence of widespread broken formation (Lapierre, 1972; Robertson & Woodcock, 1979; Swarbrick, 1980). Differences include: (1) an absence of neritic carbonates, other than blocks of Late Triassic limestone (Petra tou Romiou Limestone) interpreted as oceanic seamounts; (2) the presence of Triassic terrigenous sandstone turbidites without volcanic rocks, in contrast to the mixed terrigenous–volcanogenic units of the Mersin Melange; (3) an absence of emplacement related gravity deposits, other than locally overlying, undeformed debris flow deposits (Kathikas Melange: Swarbrick & Naylor, 1979); (4) an absence of an over-riding ophiolite and metamorphic sole. Ophiolitic and related metamorphic rocks occur in high-angle fault contact with Triassic–Cretaceous sedimentary and volcanic rocks of continental margin to oceanic affinities, respectively (Robertson & Xenophontos, 1993). The Mamonia Complex is restored as part of the rifted southern margin of the Tauride Carbonate Platform, or of a satellite microcontinent (Robertson, 1998, 2000).

The Antalya Complex, southern Turkey, includes continental margin and oceanic units of similar age to the Mersin Melange. The exposures of the Antalya Complex nearest to the Mersin Melange are located within the elongate Güzelsu Corridor, between the Tauride Carbonate Platform to the north and the

https://doi.org/10.1017/S0016756804009094 Published online by Cambridge University Press

metamorphic Alanya Massif to the south (Fig. 1). Differences with the Mersin Melange include: (1) the Antalya sedimentary succession in this area is associated with thick (*c*. 1000 m) intact successions of coralgal limestone of mainly Late Triassic age (e.g. Katran Dağ: Monod, 1977). These neritic carbonates are much thicker and more intact than the Triassic neritic broken formation of the Mersin Melange; (2) Triassic basalts exposed in the Güzelsu corridor are of WPB type (Robertson & Waldron, 1990), in contrast to the siliceous extrusive and tuffaceous rocks of the Mersin Melange; (3) Late Triassic quartzose turbidites pass upwards into Late Triassic hemi-pelagic Halobia limestone, then radiolarites of Late Jurassic–Early Cretaceous age, and local Cretaceous pelagic carbonates (very locally preserved). Ammonitico Rosso is not present in contrast to the Mersin Melange (and the Beyşehir–Hoyran Nappes). Similar, but much more extensive, exposures of the Antalya Complex are present in the Isparta Angle further west (Poisson, 1977; Robertson & Woodcock, 1982; Robertson *et al*. 1991; Robertson, Poisson & Akinci, 2003). The Mesozoic succession of the Antalya Complex exhibits many similarities with the Mamonia Complex of western Cyprus and is interpreted as forming part of the rifted southern margin of the Tauride Carbonate Platform, which was divided into several carbonate platforms separated by basins (Robertson, 1998, 2000).

13. Discussion: direction of emplacement

The regional comparisons, outlined above, support derivation of the Mersin Melange from Neotethys to the north of the Tauride Carbonate Platform.

(1) The Mersin Melange is similar in age and restored stratigraphy to the Beyşehir–Hoyran Nappes that are generally accepted to have been emplaced southwards onto the Tauride Carbonate Platform, initially in latest Cretaceous time (Monod, 1977; Özgül, 1984, 1997; Andrew & Robertson, 2002). (2) There is kinematic evidence that the Pozantı–Karsantı ophiolite and related units (Parlak, Höck & Delaloye, 2002), located along the northern margin of the Tauride Carbonate Platform, were emplaced southwards onto the Tauride Carbonate Platform (Polat & Casey, 1995) (that is, towards the Mersin Melange and ophiolite exposures). (3) Ophiolites and melange were thrust southwards over Tauride Carbonate Platform-related units from a northerly Neotethyan oceanic basin. This applies across Turkey as a whole, from the Lycian Nappes in the west to the Munzur Dağ in the east (Şengör & Yılmaz, 1981; Robertson & Dixon, 1984). (4) There is limited evidence of south-facing folds in the Mersin Melange although fold facing can rarely be observed. (5) There is, at present, no convincing evidence of Late Cretaceous ophiolites being emplaced northwards over Tauride carbonate platform units in latest Cretaceous time in adjacent regions. This applies from the Antalya Complex in the west to the Bitlis suture zone in southeastern Turkey. Evidence from southeastern Turkey suggests the southern Neotethys was subducted northwards beneath the Tauride Carbonate Platform (Hall, 1977; Aktaş & Robertson, 1984; Yılmaz, 1993; Robertson *et al*. 2004). (6) Palaeozoic successions exposed in the southern part of the Tauride Carbonate Platform lack evidence of Late Palaeozoic magmatic intrusions (Demirtaşlı *et al*. 1984; Göncuöğlu & Kozlu, 2000), such that it is more probable that the dated Devonian granite was derived from further north, as discussed earlier.

However, a northerly derivation is not without several problems. (1) The Mersin Melange dips regionally southwards at a higher angle than can be explained simply by Tertiary uplift. (2) We observed northerly vergence (thrust duplexes and folds) from the basalt–radiolarite–pelagic limestone lithological association just beneath the Mersin Ophiolite and from the basal serpentinized harzburgite above. (3) We confirm that later stage brittle folds and some outcrop-scale duplexes from the metamorphic sole show mainly northward vergence (Parlak, Bozkurt & Delaloye, 1996), although, as discussed earlier, the early-stage high-temperature ductile folds do not record evidence of emplacement direction.

14. Proposed tectonic model

How can the above apparently opposing lines of structural evidence be resolved? Here, we propose that the Mersin Melange and Mersin Ophiolite were initially emplaced from the north, but then soon underwent a phase of backthrusting related to the exhumation of the Tauride Carbonate Platform from beneath the ophiolite.

During emplacement, the rift/passive margin units of the Mersin Melange and the distal edge of the Tauride Carbonate Platform were detached and emplaced together with the over-riding Mersin Ophiolite during Campanian–Maastrichtian time. By contrast, as a result of attempted northward subduction, the leading edge of the northern margin of the Tauride Carbonate Platform (Northern Bolkar Dağ unit) was underthrust, deeply buried (tens of kilometres) and metamorphosed under HP–LT conditions. As a result of the buoyancy of the downgoing continental crust this leading edge was then rapidly exhumed, allowing a sedimentary transgression of the over-riding ophiolite and ophiolitic melange still during Maastrichtian time. During post-suturing compression in Late Eocene time, the Tauride Carbonate Platform in this area was subdivided by northward thrusting into the Northern Bolkar Dağ unit and the structurally overlying Southern Bolkar Dağ unit. The Northern Bolkar Dağ unit was, in turn, thrust northwards over the Alihoca ophiolite, the related melange and the mutual Maastrichtian–Palaeogene

sedimentary–volcanic cover of both units (Jaffey & Robertson, 2001; Clark & Robertson, 2002).

After latest Cretaceous exhumation, the Mersin Melange was exposed, probably subaerially, giving rise to locally preserved, but undated, transgressive conglomerates. Considerably further southwest in a small area north of Mersin (south of Namrun), the melange is unconformably overlain by basal conglomerates, passing first into sandstones, then into Paleocene (Ilerdian) shallow-marine argillaceous limestones rich in neritic foraminifera (*Alveolina subpyrenaica*, *A. moussoulensis* and *A. varians*). The intact succession continues with sandstones, then Nummulitic limestones of Cuisian–Lutetian age, in turn unconformably overlain, above a basal conglomerate, by Lower Miocene carbonate rocks of the Adana Basin (Avşar, 1992). Later, the whole area was transgressed by shallow-water nummulitic carbonates during the Eocene–Oligocene, although only small remnants of this facies are now exposed. During Early Miocene time, the southern margin of the Tauride carbonate platform was transgressed by shallow-water carbonates, initiating the Adana Basin that was subaerially exposed by Late Miocene time. Uplift and erosion followed in Plio-Quaternary time, culminating in deep dissection to expose the Mersin Ophiolite beneath the Adana Basin.

We explain the north-verging structures associated with the Mersin Melange and the Mersin Ophiolite by backthrusting during exhumation of the partially subducted Tauride Carbonate Platform. A similar problem of anomalous thrust vergence occurs in Oman (south of the Semail Gap). Structures are indicative of the emplacement of the Oman ophiolite onto the Arabian continental margin from the NNE to SSW, regionally. However, large-scale NNE-facing recumbent sheath folds occur in HP–LT metamorphic rocks. Searle & Cox (1999) attribute these anomalous oceanward-directed structures to the exhumation of the leading edge of the Arabian passive continental margin after its subduction and metamorphism under HP–LT conditions. During Late Cretaceous time, the Oman ophiolite is considered to have formed above a northeastward-dipping intra-oceanic subduction zone (Pearce *et al*. 1981, 1984). This subduction zone is inferred to have subsequently collided with the Oman passive margin, emplacing the Oman ophiolite and the Hawasina continental margin sedimentary and volcanic rocks onto the Arabian platform (e.g. Robertson & Searle, 1990). The leading edge of the Arabian passive margin was deeply buried as a result of attempted subduction, followed by rapid exhumation, prior to the end of Cretaceous time. Large-scale, low-angle normal faults and oceanward-directed folds and thrusts formed during this exhumation in response to large-scale shear between the underthrust margin and the over-riding ophiolite.

Comparable high pressure–low temperature rocks are associated with the Tauride Carbonate Platform, north of the Mersin Melange (Dilek & Whitney, 1997). As in Oman, the emplacement of a supra-subduction ophiolite is seen as being driven by trench–margin collision, coupled with attempted subduction of the leading edge of the continental margin, in this case the Bolkar Dağ. Exhumation took place in both regions rapidly, during Maastrichtian time in both areas (Clark & Robertson, 2002; Robertson & Searle, 1990). During this exhumation, large-scale shear took place between an exhuming Tauride Carbonate Platform and a backthrusting Mersin Ophiolite, as inferred for Oman (Searle & Cox, 1999). This deformation is seen as producing the north-verging brittle structures observed, particularly near the base of the ophiolite, together with the southward inclination of the Mersin Melange as a whole. Comparable latest Cretaceous exhumation of HP/LT assemblages is known to have affected the northern margin of the Tauride Carbonate Platform (Anatolides) in western Turkey on a regional basis (Okay, Harris & Kelley, 1998).

15. Conclusions: palaeotectonic evolution

We conclude by summarizing our view of the tectonic evolution of the Mersin Melange as a series of time slices (Fig. 18).

Late Permian. Shallow-water carbonates were deposited along the northern margin of the future Tauride Carbonate Platform in a pre-rift or early-rift setting.

Early–Mid-Triassic. The rift became volcanically active, with the eruption of mainly silicic lavas and tuffs in Mid–Late Triassic time (Fig. 18a). Terrigenous sandstones and conglomerates were eroded from the Palaeozoic basement of the future Tauride Carbonate Platform and deposited within the rift, largely by turbidity currents and debris flows.

Late Triassic–Early Cretaceous. Passive margin subsidence ensued (Fig. 18b). A horst-graben topography remained after volcanism ended that was characterized by a range of shallow-water, slope and deeper water basinal settings in which mainly carbonate sediments accumulated. Submerged platforms ('highs') were overlain by stratigraphically condensed Ammonitico Rosso, by comparison with similar facies in the Beyşehir–Hoyran Nappes (Boyalı Tepe-type facies: Monod, 1977; Andrew & Robertson, 2002). These carbonates were covered by radiolarian oozes of inferred Late Jurassic–Early Cretaceous age, as in the Beyşehir–Hoyran Nappes.

Late Cretaceous. The Mersin Ophiolite formed within Neotethys (Fig. 18c) above an inferred intra-oceanic subduction zone (Parlak, Delaloye & Bingöl, 1996). A similar setting is postulated for the Beyşehir ophiolite further west (Andrew & Robertson, 2002). Pelagic carbonates were deposited over the entire region, from the platform to the adjacent oceanic crust during the Late Cretaceous.

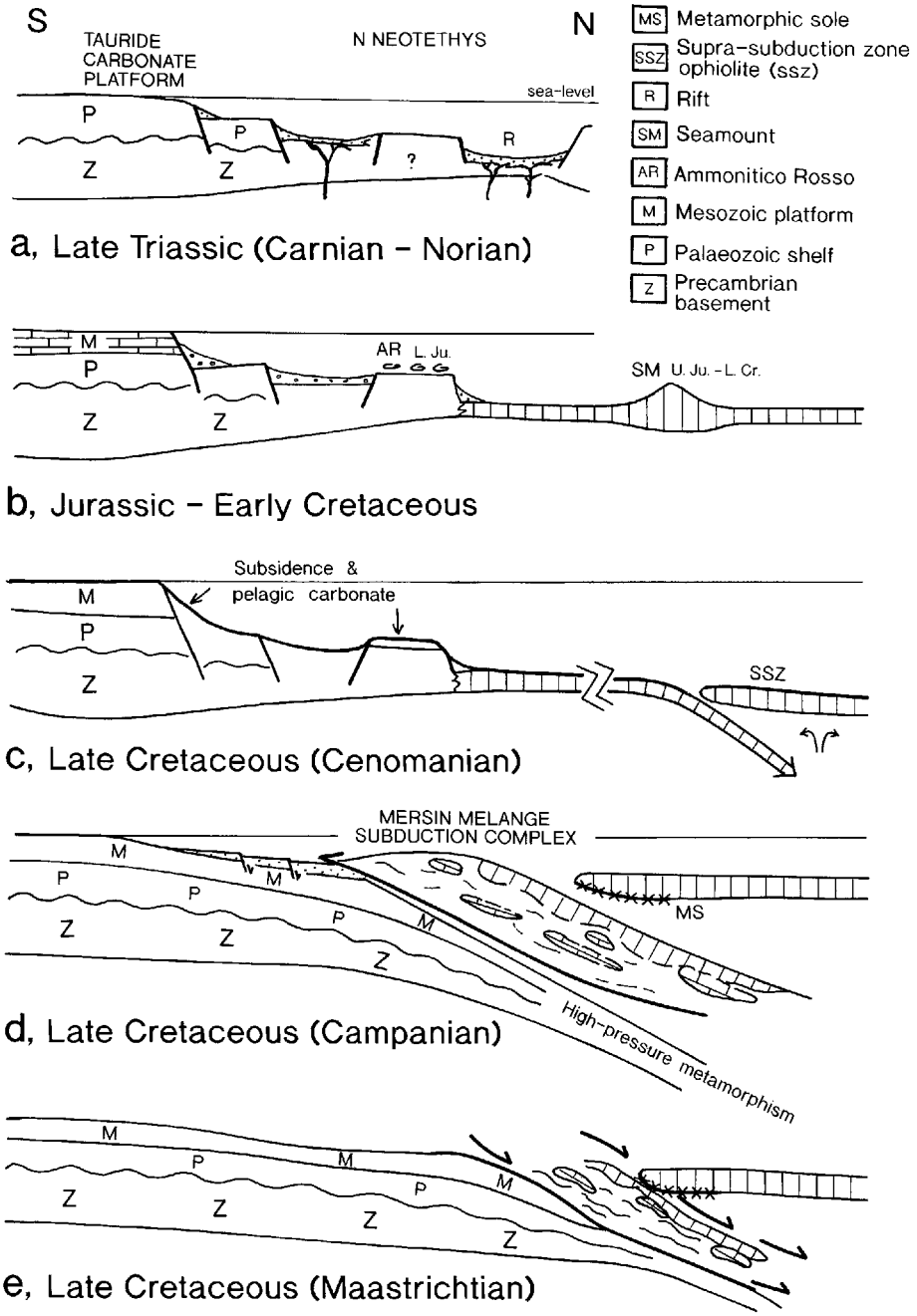

Figure 18. Plate tectonic cartoons showing the inferred development of the Mersin Melange. (a) Late Triassic rifting; (b) Jurassic–Lower Cretaceous passive margin subsidence; (c) Cretaceous supra-subduction zone (SSZ) spreading; (d) latest Cretaceous subduction–accretion of the Melange and HP–LT metamorphism of the subducted, leading edge of the Tauride Carbonate Platform; (e) latest Cretaceous exhumation and associated back-thrusting.

Northward intra-oceanic converge was initiated around 92.6 ± 0.2 Ma, giving rise to the high-temperature amphibolite facies metamorphic sole of the ophiolite (Parlak & Delaloye, 1999; Fig. 18d). The protoliths of the underplated amphibolite and greenschist facies metamorphic rocks are viewed as originally one, or several, small volcanic build-ups that were preferentially accreted, whereas the underlying oceanic crust was subducted. During subduction/accretion, sedimentary and volcanic material was reworked as debris-flow deposits and lithoclastic turbidites. These sediments probably accumulated in small thrust-top basins within the accretionary prism and were later incorporated into the accretionary wedge. The main driving force of southward emplacement of the ophiolite and melange was the collision of the leading edge of the Tauride continental margin with the subduction trench. The northern margin of the Tauride Carbonate Platform was simultaneously deeply buried and metamorphosed up to HP–LT conditions.

https://doi.org/10.1017/S0016756804009094 Published online by Cambridge University Press

Rapid exhumation of the platform is inferred to have given rise to northward-verging brittle-type structures locally affecting the base of the ophiolite, the metamorphic sole and the underlying Mersin Melange. After exhumation the Tauride Carbonate Platform was transgressed prior to the end of Maastrichtian time.

Acknowledgements. The first author thanks Prof. Michel Delaloye for making available laboratory facilities at the Univesity of Geneva, Switzerland. We also thank Fabio Capponi and Jean Claude Lavanchy (University of Geneva) for assisting with the major and trace element analyses. The second author thanks Diana Baty for assistance with drafting some of the figures and Yvonne Cooper for preparing the photographic plates. Helpful reviews of the manuscript were received from Drs P. Floyd and A. Morris. The first author thanks TUBA (Turkish Academy of Sciences) for financial support.

References

AKTAŞ, G. & ROBERTSON, A. H. F. 1984. The Maden Complex, SE Turkey: Evolution of a Neo-Tethyan active margin. In *The Geological Evolution of the Eastern Mediterranean* (eds J. E. Dixon and A. H. F. Robertson), pp. 375–402. Geological Society of London, Special Publication no. 17.

AL-RIYAMI, K. & ROBERTSON, A. H. F. 2002. Mesozoic sedimentary and magmatic evolution of the Arabian continental margin, northern Syria: evidence from the Baer–Bassit Melange. *Geological Magazine* **139**, 395–420.

AMERICAN GEOLOGICAL INSTITUTE. 1961. *Dictionary of Geological Terms*. New York: Dolphin Books.

ANDREW, T. & ROBERTSON, A. H. F. 2002. Beyşehir–Hoyran–Hadim Nappes: genesis and emplacement of Mesozoic marginal and oceanic units of the Northern Neotethys in Southern Turkey. *Journal of the Geological Society, London* **159**, 529–43.

ARCULUS, R. J. & POWEL, R. 1986. Source component mixing in the regions of arc magma generation. *Journal of Geophysical Research* **91**, 5913–26.

AVŞAR, N. 1992. Namrun (İçel) yöresi Paleojen bentik foraminifer faunası. *Maden Tetkik ve Arama Dergisi* **114**, 127–44.

ÇAKIR, Ü. 1978. *Pétrologie du massif ophiolitique de Pozantı–Karsantı (Taurus cilicien, Turquie): Etude de la partie centrale*. Thèse troisième cycle, Strasbourg, France, Université Louis Pasteur, 251 pp.

CLARK, M. & ROBERTSON, A. H. F. 2002. The role of the Early Tertiary Ulukışla Basin, southern Turkey, in suturing of the Mesozoic Tethys ocean. *Journal of the Geological Society, London* **159**, 673–90.

COLLINS, A. & ROBERTSON, A. H. F. 1997. Lycian mélange, southwestern Turkey: an emplaced Late Cretaceous accretionary complex. *Geology* **25**, 255–8.

COLLINS, A. S. & ROBERTSON, A. H. F. 1998. Processes of late Cretaceous to late Miocene episodic thrust-sheet translation in the Lycian Taurides, SW Turkey. *Journal of the Geological Society, London* **155**, 759–72.

COX, K. G., BELL, J. D. & PANKHURST, R. J. 1979. *The Interpretation of Igneous Rocks*. London: Allen and Unwin.

CULLERS, R. L. & GRAF, J. L. 1984. Rare earth element in igneous rocks of the continental crust: intermediate and silicic rocks-ore petrogenesis. In *REE Geochemistry* (ed. P. Henderson), pp. 275–308. Amsterdam: Elsevier.

DEER, W. A., HOWIE, R. A. & ZUSSMAN, J. 1992. *An Introduction to the Rock Forming Minerals*. Longman Scientific and Technical.

DE GRACIANCKY, P. C. 1972. *Récherchers géologiques dans les Taurus Lycien*. (Thèse D. Sc.) Université de Paris Sud, France.

DELALOYE, M. & WAGNER, J. J. 1984. Ophiolites and volcanic activity near the western edge of the Arabian plate. In *The Geological Evolution of the Eastern Mediterranean* (eds J. E. Dixon and A. H. F. Robertson), pp. 225–33. Geological Society of London, Special Publication no. 17.

DELAUNE-MAYÈRE, M. 1984. Evolution of a Mesozoic passive continental margin: Bear–Bassit (NW Syria). In *The Geological Evolution of the Eastern Mediterranean* (eds J. E. Dixon and A. H. F. Robertson), pp. 151–9. Geological Society of London, Special Publication no. 17.

DEMİRTAŞLI, E., TURHAN, N., BİLGİN, A. Z. & SELİM, M. 1984. Geology of the Bolkar Mountains. In *Geology of the Taurus Belt* (eds O. Tekeli and M. C. Göncüoğlu), pp. 125–41. Proceedings of International Symposium on the Geology of the Taurus Belt, 1983. Ankara, Turkey.

DERCOURT, J., RICOU, L. E. & VRIELYNCK, B. (eds) 1993. Atlas Tethys Paleoenvironmental Maps, Beicip-Franlab.

DE WEVER, P. 1989. Radiolarians, radiolarites, and Mesozoic paleogeography of the Circum-Mediterranean Alpine Belts. In *Siliceous deposits of the Tethys and Pacific regions* (eds J. R. Hein and J. Obradovic), pp. 31–50. Springer.

DİLEK, Y., THY, P., HACKER, B. & GRUNDVIG, S. 1999. Structure and petrology of Tauride ophiolites and mafic dyke intrusions (Turkey): implications for the Neotethyan ocean. *Geological Society of America Bulletin* **111**, 1192–1216.

DİLEK, Y. & WHITNEY, D. L. 1997. Counterclockwise P–T–t trajectory from the metamorphic sole of a Neotethyan ophiolite (Turkey). *Tectonophysics* **280**, 295–310.

DİLEK, Y. & WHITNEY, D. L. 2000. Cenozoic evolution in Central Anatolia: extension, magmatism and landscape development. In *Proceedings 3rd International Conference on the Geology of the Eastern Mediterranean* (eds I. Panayides, C. Xenophontos and J. Malpas), pp. 183–92. Geological Survey Department, Nicosia, Cyprus.

ELİTOK, Ö. 2002. Geochemistry and tectonic significance of the Şarkikaraağaç Ophiolite in the Beyşehir–Hoyran Nappes, S. W. Turkey. In *Proceedings of 4th International Symposium on Eastern Mediterranean Geology*, pp. 181–96. Isparta, Turkey.

FLOYD, P. A. & WINCHESTER, J. A. 1975. Magma type and tectonic setting discrimination using immobile elements. *Earth and Planetary Science Letters* **27**, 211–18.

FLOYD, P. A. & WINCHESTER, J. A. 1978. Identification and discrimination of altered and metamorphosed volcanic rocks using immobile elements. *Chemical Geology* **21**, 291–306.

GANSSER, A. 1974. The ophiolitic mélange, a world-wide problem on Tethyan examples. *Eclogae Geologicae Helvetiae* **67**, 479–507.

GÖNCÜOĞLU, M. C. & KOZLU, H. 2000. Early Paleozoic evolution of the NW Gondwanaland: Data from Southern Turkey and surrounding regions. *Gondwana Research* **3**, 315–24.

HALL, R. 1977. Ophiolite emplacement and the evolution of the Taurus suture zone, south-east Turkey. *Bulletin of the Geological Society of America* **87**, 1078–88.

HALL, R. 1980. Unmixing a mélange: the petrology and history of a disrupted and metamorphosed ophiolite, SE Turkey. *Journal of the Geological Society, London* **137**, 195–206.

HARRIS, N. B. W., PEARCE, J. A. & TINDLE, A. G. 1986. Geochemical characteristics of collision-zone magmatism. In *Collision Tectonics* (eds M. P. Coward and A. C. Ries), pp. 67–81. Geological Society of London, Special Publication no. 19.

HART, R. A. 1970. Chemical exchange between seawater and deep ocean basalts. *Earth and Planetary Science Letters* **9**, 269–79.

HUMPHRIS, S. E. & THOMPSON, G. 1978. Trace element mobility during hydrothermal alteration of oceanic basalts. *Geochimica et Cosmochimica Acta* **42**, 127–36.

IRVINE, T. N. & BARAGAR, W. R. A. 1971. A guide to the chemical classification of the common volcanic rocks. *Canadian Journal of Earth Sciences* **8**, 523–48.

JAFFEY, N. & ROBERTSON, A. H. F. 2001. New sedimentoloical and structural data from the Ecemiş Fault Zone, southern Turkey; implications for its timing and offset and the Cenozoic tectonic escape of Anatolia. *Journal of the Geological Society, London* **18**, 367–78.

JAKES, P. & GILL, J. 1970. Rare earth elements and the island arc tholeiitic series. *Earth and Planetary Science Letters* **9**, 17–28.

JENKYNS, H. C. & WINTERER, E. L. 1982. Palaeoceanography of Mesozoic ribbon radiolarites. *Earth and Planetary Science Letters* **60**, 351–75.

JUTEAU, T. 1980. Ophiolites of Turkey. *Ofioliti* **2**, 199–238.

KRÖNER, A. & ŞENGÖR, A. M. C. 1990. Archean and Proterozoic ancestry in lower Pre-Cambrian to early Palaeozoic crustal elements of southern Turkey as revealed by single zircon dating. *Geology* **18**, 1186–90.

LAPIERRE, H. 1972. *Les formations sédimentaires et éruptives des nappes de Mamonia et leurs relations avec le massif de Troodos (Chypre)*. Thèse Doctoral, Univ. Nancy, France (published thesis).

LYTWYN, J. N. & CASEY, J. F. 1995. The geochemistry of postkinematic mafic dyke swarms and subophiolitic metabasites, Pozantı–Karsantı ophiolite, Turkey: evidence for ridge subduction. *Geological Society of America Bulletin* **107**, 830–50.

MESCHEDE, M. 1986. A method of discriminating between different types of mid-oceanic ridge basalts and continental tholeiites with Nb–Zr–Y diagram. *Chemical Geology* **56**, 207–18.

MILLER, C. F. & STODDARD, E. F. 1981. The role of manganese in the paragenesis of magmatic garnet: an example from the Old-Woman-Piute range, California. *Journal of Geology* **89**, 233–46.

MIYASHIRO, A. 1978. Nature of alkalic rocks series. *Contributions to Mineralogy and Petrology* **66**, 91–104.

MONOD, O. 1977. *Récherches géologiques dans les Taurus occidental au sud de Beyşehir (Turquie)*. Thèse de Doctoral, Université de Paris-Sud, Orsay (published thesis).

MONOD, O. & AKAY, E. 1984. Evidence for Upper Triassic–early Jurassic orogenic event in the Taurides. In *The Geological Evolution of the Eastern Mediterranean* (eds J. E. Dixon and A. H. F. Robertson), pp. 113–28. Geological Society of London, Special Publication no. 17.

MORRIS, A., ANDERSON, M., ROBERTSON, A. H. F. & AL-RIYAMI, K. 2002. Extreme tectonic rotations within an eastern Mediterranean ophiolite (Baer-Basasit, Syria). *Earth and Planetary Science Letters* **202**, 247–61.

OKAY, A. I., HARRIS, N. B. W. & KELLEY, S. P. 1998. Exhumation of blueschists along a Tethyan suture in northwest Turkey. *Tectonophysics* **285**, 275–99.

ÖZGÜL, N. 1984. Stratigraphy and tectonic evolution of the central Taurides. In *Geology of the Taurus Belt* (eds O. Tekeli and M. C. Göncüoğlu), pp. 77–90. Proceedings of International Symposium on the Geology of the Taurus Belt, 1983. Ankara, Turkey.

ÖZGÜL, N. 1997. Stratigraphy of the tectono-stratigraphic units in the region Bozkır–Hadim–Taşkent (northern central Taurides) (in Turkish). *Maden Tetkik ve Arama Dergisi* **119**, 113–74.

PAMPAL, S. 1984. Arslanköy–Tepeköy (Mersin) yöresinin jeolojisi. *Selçuk Üniversitesi Fen-Edebiyat Fakültesi Fen Dergisi* **3**, 247–58.

PAMPAL, S. 1987. Güzeloluk-Sorgun (Mersin) yöresinin jeolojisi. *Gazi Üniversitesi Mühendislik-Mimarlık Fakültesi Dergisi* **2**, 143–74.

PARLAK, O. 1996. Geochemistry and geochronology of the Mersin Ophiolite within the eastern Mediterranean tectonic frame (southern Turkey). *Terre & Environment* **6**, Université de Geneve, 242 pp. (published Ph.D. thesis).

PARLAK, O. 2000. Geochemistry and significance of mafic dyke swarms in the Pozantı–Karsantı ophiolite (southern Turkey). *Turkish Journal of Earth Sciences* **24**, 29–38.

PARLAK, O., BOZKURT, E. & DELALOYE, M. 1996. Obduction direction of the Mersin Ophiolite: structural evidence from the subophiolitic metamorphics in the central Taurus Belt, southern Turkey. *International Geology Review* **38**, 778–86.

PARLAK, O., ÇELİK, Ö. F. & DELALOYE, M. 2001. Geochemistry of the volcanic rocks from the Pozantı–Karsanı ophiolite (S. Turkey). In *4th International Turkish Geology Symposium (ITGS-IV), 24–28 September 2001, Adana-Turkey*, p. 239.

PARLAK, O. & DELALOYE, M. 1996. Geochemistry and timing of post-metamorphic dyke emplacement in the Mersin Ophiolite (Southern Turkey): new age constraints from $^{40}Ar/^{39}Ar$ geochronology. *Terra Nova* **8**, 585–92.

PARLAK, O. & DELALOYE, M. 1999. Precise $^{40}Ar/^{39}Ar$ ages from the metamorphic sole of the Mersin Ophiolite (southern Turkey). *Tectonophysics* **301**, 145–58.

PARLAK, O., DELALOYE, M. & BİNGÖL, E. 1995. Origin of sub-ophiolitic metamorphic rocks beneath the Mersin Ophiolite, Southern Turkey. *Ofioliti* **20**, 97–110.

PARLAK, O., DELALOYE, M. & BİNGÖL, E. 1996. Mineral chemistry of ultramafic and mafic cumulates as an indicator of the arc-related origin of the Mersin Ophiolite (southern Turkey). *Geologische Rundschau* **85**, 647–61.

PARLAK, O., DELALOYE, M. & BİNGÖL, E. 1997. Geochemistry of the volcanic rocks in the Mersin Ophiolite (southern Turkey) and their tectonic significance in the eastern Mediterranean geology. In *Proceedings of International Earth Science Colloquium on the Aegean region-IESCA 1995* (eds Ö. Pişkin, M. Ergün, M. Y. Savaşçın and G. Tarcan), pp. 441–63. Dokuz Eylül University, İzmir, Turkey.

PARLAK, O., HÖCK, V. & DELALOYE, M. 2000. Supra-subduction zone origin of the Pozantı–Karsantı ophiolite (southern Turkey) deduced from whole-rock and mineral

chemistry of the gabbroic cumulates. In *Tectonics and Magmatism in Turkey and the Surrounding Area* (eds E. Bozkurt, J. A. Winchester and J. D. A. Piper), pp. 219–34. Geological Society of London, Special Publication no. 173.

PARLAK, O., HÖCK, V. & DELALOYE, M. 2002. The suprasubduction zone Pozantı–Karsantı ophiolite, southern Turkey: evidence for high-pressure crystal fractionation of ultramafic cumulates. *Lithos* **65**, 205–24.

PARROT, J. F. 1977. Assemblage ophiolitique de Baer-Bassit et termes éffusives du volcano-sédimentaire. *Travaux et Documents de L'O. R. S. T. R. O. M.* **72**, 333 pp.

PEACOCK, M. A. 1931. Classification of igneous rock series. *Journal of Geology* **39**, 65–7.

PEARCE, J. A. 1982. Trace element characteristics of lavas from destructive plate boundaries. In *Andesites* (ed. R. S. Thorpe), pp. 525–48. New York: Wiley.

PEARCE, J. A., ALABASTER, T., SHELTON, A. W. & SEARLE, M. P. 1981. The Oman ophiolite as a Cretaceous arc-basin complex: evidence and implications. *Philosophical Transactions of the Royal Society of London* **A300**, 299–317.

PEARCE, J. A. & CANN, J. R. 1973. Tectonic setting of basaltic volcanic rocks determined using trace element analysis. *Earth and Planetary Science Letters* **19**, 290–300.

PEARCE, J. A., HARRIS, B. W. & TINDLE, A. G. 1984. Trace element discrimination diagrams for the tectonic interpretation of granitic rocks. *Journal of Petrology* **25**, 956–83.

PEARCE, J. A., LIPPARD, S. J. & ROBERTS, S. 1984. Characteristics and tectonic significance of suprasubduction zone ophiolites. In *Marginal Basin Geology* (eds B. P. Kokelaar and M. F. Howells), pp. 77–89. Geological Society of London, Special Publication no. 16.

PEARCE, J. A. & NORRY, M. J. 1979. Petrogenetic implications of Ti, Zr, Y and Nb variations in volcanic rocks. *Contributions to Mineralogy and Petrology* **69**, 33–47.

PERFIT, M. R., GUST, D. A., BENCE, A. E., ARCULUS, R. J. & TAYLOR, S. R. 1980. Chemical characteristics of island arc basalts: implications for mantle sources. *Chemical Geology* **30**, 227–56.

POISSON, A. 1977. Récherches géologiques dans les Taurides occidentales, Turquie. Thèse de Doctoral, Univ. Paris-Sud, Orsay, France (published thesis).

POLAT, A. & CASEY, J. F. 1995. A structural record of the emplacement of the Pozantı–Karsantı ophiolite onto the Menderes–Taurus block in the Late Cretaceous, eastern Taurides, Turkey. *Journal of Structural Geology* **17**, 1673–88.

POLAT, A., CASEY, J. F. & KERRICH, R. 1996. Geochemical characteristics of accreted material beneath the Pozantı–Karsantı ophiolite, Turkey: Intra-oceanic detachment, assembly and obduction. *Tectonophysics* **263**, 249–76.

PRICE, I. 1977. Facies distinction and interpretation of primary cherts in a Mesozoic continental margin succession, Othris (Greece). *Journal of Sedimentary Petrology* **18**, 321–35.

RAYMOND, L. A. 1984. (ed.) *Melanges: Their Nature, Origin and Significance.* Geological Society of America, Special Paper no. 198.

RICOU, L. E., ARGYRIADIS, I. & MARCOUX, J. 1975. L'axe calcaire du Taurus, une alignement de fenêtres arabo-africaines sous des nappes radiolaritique, ophiolitiques et métamorphiques. *Bulletin de la Société géologique de France* **17**, 1024–43.

ROBERTSON, A. H. F. 1994. Role of the tectonic facies concept in orogenic analysis and its application to Tethys in the Eastern Mediterranean region. *Earth Science Reviews* **37**, 139–213.

ROBERTSON, A. H. F. 1998. Mesozoic–Tertiary tectonic evolution of the easternmost Mediterranean area: integration of marine and land evidence. In *Proceedings of the Ocean Drilling Program, Scientific Results, vol. 160* (eds A. H. F. Robertson, K. C. Emeis, K. C. Richter and A. Camerlenghi), pp. 723–82. College Station, Texas.

ROBERTSON, A. H. F. 2000. Mesozoic–Tertiary tectonic-sedimentary evolution of a south Tethyan oceanic basin and its margins in southern Turkey. In *Tectonics and Magmatism in Turkey and the Surrounding Area* (eds E. Bozkurt, J. A. Winchester and J. D. A. Piper), pp. 43–82. Geological Society of London, Special Publication no. 173.

ROBERTSON, A. H. F. 2002. Overview of the genesis and emplacement of Mesozoic ophiolites in the Eastern Mediterranean Tethyan region. *Lithos* **65**, 1–68.

ROBERTSON, A. H. F., CLIFT, P. D., DEGNAN, P. J. & JONES, G. 1991. Palaeogeographical and palaeotectonic evolution of the eastern Mediterranean Neotethys. *Palaeoceanography Palaeclimatology Palaeoecology* **87**, 289–343.

ROBERTSON, A. H. F. & DEGNAN, P. 1998. Significance of modern and ancient oceanic Mn-rich hydrothermal sediments, exemplified by Jurassic Mn-cherts from Southern Greece. In *Modern Ocean Floor Processes and the Geological Record* (eds R. A. Mills and K. Harrison), pp. 217–40. Geological Society of London, Special Publication no. 148.

ROBERTSON, A. H. F. & DIXON, J. E. 1984. Introduction: aspects of the geological evolution of the Eastern Mediterranean. In *The geological evolution of the Eastern Mediterranean* (eds J. E. Dixon and A. H. F. Robertson), pp. 1–74. Geological Society of London, Special Publication no. 17.

ROBERTSON, A. H. F., POISSON, A. & AKINCI, Ö. 2003. Developments in research concerning the Mesozoic–Tertiary Tethys and neotectonics in the Isparta Angle, SW Turkey. *Geological Journal* **38**, 195–234.

ROBERTSON, A. H. F. & SEARLE, M. P. 1990. The northern Oman Tethyan continental margin: stratigraphy, structure, concepts and controversies. In *The Geology and Tectonics of the Oman Region* (eds A. H. F. Robertson, M. P. Searle and A. C. Ries), pp. 3–25. Geological Society of London, Special Publication no. 49.

ROBERTSON, A. H. F., ÜNLÜGENÇ, U., İNAN, N. & TASLI, K. 2004. The Misis-Andırın Complex: a Mid-Tertiary mélange related to late-stage subduction of the Southern Neotethys in S Turkey. *Journal of Asian Earth Sciences*, **22**, 413–453.

ROBERTSON, A. H. F. & WALDRON, J. W. F. 1990. Geochemistry and tectonic setting of Late Triassic and Late Jurassic–Early Cretaceous basaltic extrusives from the Antalya Complex, SW Turkey. In *Proceedings of International Earth Science Congress on Aegean Regions* (eds M. Y. Savaşçın and A. H. Eronat), pp. 279–99. Izmir, Turkey.

ROBERTSON, A. H. F. & WOODCOCK, N. H. 1979. Mamonia Complex, southwest Cyprus: Evolution and emplacement of a Mesozoic continental margin. *Geological Society of American Bulletin* **90**, 651–65.

ROBERTSON, A. H. F. & WOODCOCK, N. H. 1982. Sedimentary history of the south-western segment of the Mesozoic–Tertiary Antalya continental margin,

south-western Turkey. *Eclogae Geologica Helvetiae* **75**, 517–62.

ROBERTSON, A. H. F. & XENOPHONTOS, C. 1993. Development of concepts concerning the Troodos ophiolite and adjacent units in Cyprus. In *Magmatic Processes and Plate Tectonics* (eds H. M. Prichard, T. Alabaster, N. B. W. Harris and C. R. Neary), pp. 85–119. Bath: Geological Society of London, Special Publication no. 76.

SEARLE, M. P. & COX, J. 1999. Tectonic setting, origin and obduction of the Oman ophiolite. *Geological Society of American Bulletin* **111**, 104–22.

ŞENEL, Y. M. 1991. Palaeocene–Eocene sediments interbedded with volcanics within the Lycian Nappes: Faralya Formation. *Bulletin of Mineral Research and Exploration* **113**, 1–14.

ŞENGÖR, A. M. C. & YILMAZ, Y. 1981. Tethyan evolution of Turkey: a plate tectonic approach. *Tectonophysics* **75**, 81–241.

SHAND, S. J. 1951. *Eruptive Rocks*. New York: J. Wiley.

STAMPFLI, G., MOSAR, J., FAURE, P., PILLEVUIT, A. & VANNAY, J.-C. 2001. Permo-Mesozoic evolution of the western Tethys real: the Neotehys East Mediterranean basin connection. In *Peri-Tethys Memoir no. 5, Peri-Tethyan Rift/Wrench Basins and Passive Margins* (eds P. Ziegler, W. Cavazza, A. H. F. Robertson and S. Crasquin-Soleau), pp. 51–108. Memoirs du Museum National D'Histoire Naturelle.

STEIGER, R. H. & JÄGER, E. 1977. Subcomission on geochronology: convention on the use of decay constants in geo- and cosmochronology. *Earth and Planetary Science Letters* **36**, 359–62.

SUN, S.-S. & MCDONOUGH, W. F. 1989. Chemical and isotopic systematics of oceanic basalts: implications for mantle composition and processes. In *Magmatism in the Ocean Basins* (eds A. D. Saunders and M. J. Norry), pp. 313–45. Geological Society of London, Special Publication no. 42.

SWARBRICK, R. E. 1980. The Mamonia Complex of S. W. Cyprus: A Mesozoic continental margin and its relationship with the Troodos Complex. In *Proceedings of International Ophiolite Symposium* (ed. A. Panayiotou), pp. 86–92. 1979, Nicosia, Cyprus.

SWARBRICK, R. E. & NAYLOR, M. 1979. The Kathikas Melange, southwest Cyprus: late Cretaceous submarine debris flows. *Sedimentology* **27**, 63–78.

TEKELİ, O., AKSAY, A., URGUN, B. M. & IŞLIK, A. 1984. Geology of the Aladağ Mountains. In *Geology of the Taurus Belt* (eds O. Tekeli and M. C. Göncüoğlu), pp. 143–58. Proceedings of International Symposium on the Geology of the Taurus Belt, 1983, Ankara, Turkey.

TEKELİ, O. & ERENDİL, M. 1986. Geology and Petrology of the Kizildağ ophiolite (Hatay). *Bulletin of the Mineral Research and Exploration Institute* **21**, 21–37.

THOMPSON, G. 1973. A geochemical study of the low temperature interaction of seawater and oceanic igneous rocks. *Transactions of the American Geophysical Union* **54**, 1015–19.

VOLDET, P. 1993. From neutron activation to inductively coupled plasma-atomic emission spectrometry in the determination of rare-earth elements in rocks. *Trends in Analytical Chemistry* **12**, 339–44.

WALLIN, E. T. & METCALF, R. V. 1998. Supra-subduction zone ophiolites formed in an extensional forearc: Trinity Terrane, Klamath Mountains, California. *Journal of Geology* **106**, 591–608.

WHITECHURCH, H. 1977. *Les roches métamorphiques infraperiditotiques du Baer-Bassit (NW Syrien), temoins de l'écaillage intraocéanique téthysien. Etude pétrologique et structurale*. Thèse, Université de Nancy, France, 194 pp.

WINCHESTER, J. A. & FLOYD, P. A. 1977. Geochemical discrimination of different magma series and their differentiation products using immobile elements. *Chemical Geology* **20**, 325–43.

WOOD, D. A., JORON, J. L. & TREUIL, M. 1979. A reappraisal of the use of trace elements to classify and discriminate between magma series erupted in different tectonic settings. *Earth and Planetary Science Letters* **45**, 326–36.

YALINIZ, K. M., FLOYD, P. & GÖNCÜOĞLU, M. C. 1996. Supra-subduction zone ophiolites of Central Anatolia: geochemical evidence from the Sarikaraman ophiolite, Aksaray, Turkey. *Mineralogical Magazine* **60**, 697–710.

YILMAZ, Y. 1993. New evidence and model on the evolution of the southeast Anatolian orogen. *Geological Society of America Bulletin* **105**, 251–71.

YOGODZINSKI, G. M., VOLYNETS, O. N., KOLOSKOV, A. V., SELIVERSTOV, N. I. & MATVENKOV, V. V. 1993. Magnesian andesites and the subduction component in strongly calc-alkaline series at Piip volcano, far western Aleutians. *Journal of Petrology* **35**, 163–204.